Design of a Multi-axis Force Transducer with Applications in Track and Field

by

Zachary J. Traina

Submitted to the Department of Mechanical Engineering
in Partial Fulfillment of the Requirements for the Degree of

Bachelor of Science

at the

Massachusetts Institute of Technology

June 2005

Signature of Author .....
Department of Mechanical Engineering
May 6, 2005

Certified by .....
Warren Seering
Professor of Mechanical Engineering
Thesis Supervisor

Accepted by .....
Professor Ernest G. Cravalho
Chairman of the Undergraduate Thesis Committee

Design of a Multi-Axis Force Transducer with
Applications in Track and Field

by

Zachary J. Traina

Submitted to the Department of Mechanical Engineering
on May 6, 2005 in Partial Fulfillment of the Requirements
for the Degree of Bachelor of Science in
Mechanical Engineering

ABSTRACT

The objective of this thesis is the design and implementation of a multi-axis force transducer to be integrated into a set of track and field starting blocks. The feedback from this transducer can be used by athletes and coaches to analyze race starts, with the intention of maximizing the runner's speed and power while decreasing wasted side loads and torques. This thesis describes the design of the transducer itself and the supporting infrastructure that connects it to an existing pair of track starting blocks. The transducer is tested in several field trials and generates a measurable voltage output that varies linearly with applied load and loading position. Data collected from the field trials is further analyzed to give insight into the starting mechanics of a collegiate sprinter.

Thesis Supervisor: Warren Seering
Title: Professor of Mechanical Engineering

Acknowledgements

Many thanks to my advisor Prof. Warren Seering who has guided the design process from start to finish.

Also thanks to Dr. Barbara Hughey, who offered both her time and expertise with strain gages and measurementation circuitry, in addition to the lab equipment that was used to validate the final design.

Finally, thanks to the technical instructors and shop staff who were able to offer their expertise with manufacturing and machining the prototype: the Pappalardo Shop Staff: Dick Fenner, Bob Nuttal, Joe Cronin, Bob Gertsin, and Steve Heberek, the Edgerton Student Shop Staff, Fred Cote, and the Geld Aero Astro Machine Shop staff, Todd Billings.

Table of Contents

List of Figures

Introduction

"A lot of people run a race to see who's the fastest. I run to see who has the most guts."

- Steve Prefontaine

1.1 Background

Track blocks are used by sprinters of all skill levels as a means of increasing their speed at the start of a race. Blocks provide a vertical surface that the runner can push off of to increase his forward momentum. Without blocks, athletes are more likely to push upwards than forwards, wasting energy that could be spent increasing forward drive. The 100m sprint, the Olympic event that determines the world's "fastest man", is over in less than 10 seconds, with the winner frequently edging out his competition by less than a tenth of a second. With up to a quarter second spent in the blocks and the first few seconds of the race depending intimately on the runner's position and balance during that quarter second, the start is one of the most highly scrutinized aspects of a sprinter's race.

At the college and high school level, starts are coached by direct observation. This system incorporates a great deal of subjectivity, as advice varies from one coach to the next. An athlete might train for four years under his High School coach only to receive radically different advice from a college or professional coach. Each has an opinion on what a "fast" start is, drawn from personal experience and observation of established professional sprinters. Typically a coach will teach certain starting mechanics without any evidence for that seemingly arbitrary choice, other than the fact that his past athletes have always improved over the course of their careers. However, with so many physical and mental factors affecting an athlete's performance, it is hard to say if a sprinter is excelling because of or in spite of his start. Even if a coach is operating with fundamentally valid information, there's nothing to suggest that one methodology works best for all runners. What works for a tall athlete, for example, might not work for a stronger, shorter athlete.

Of course, there is no way to rewind an athlete's career to find out if a different starting style would have worked better. There can be no real scientific work on running mechanics in the sense that one could change a single variable and observe its effect, because the environment cannot be held constant. The athlete ages and his body changes, and he cannot be untrained. Therefore, coaches are limited to observing trends among their athletes and over time. They are able to develop speculation about which theories are valid and which are myth, but none of this speculation can amount to more than creative idea generation without objective feedback. A force measurement system offers objective feedback that no other system can provide. All subjective analysis aside, the greatest indicator of the quality of a start is how much force an athlete can put on the ground, and that information can be measured reliably and accurately for every start.

1.2 Prior Work

Of the many athletics equipment manufacturers that produce starting blocks, only Lynx System Developers, Inc has integrated electronics to give feedback about the characteristics of an athlete's start. Lynx's system, called ReacTime, offers limited feedback via an accelerometer that attaches to the back of a standard set of blocks.

In a competition setting, this feedback is limited to false start detection, allowing race officials to disqualify athletes who attempt to "jump the gun" by illegally starting too early. Lynx's system offers more detailed information such as peak force and force duration that can be recorded and reviewed after a practice session. However, because this information is offered in abstract units it is of limited value unless an athlete wishes to compare one start to the next. Additionally, the system is comprised of several independent components connected by a maze of wiring (not shown). Long and complicated set up time and the need for a PC to view the results makes using the system on a daily basis impractical.

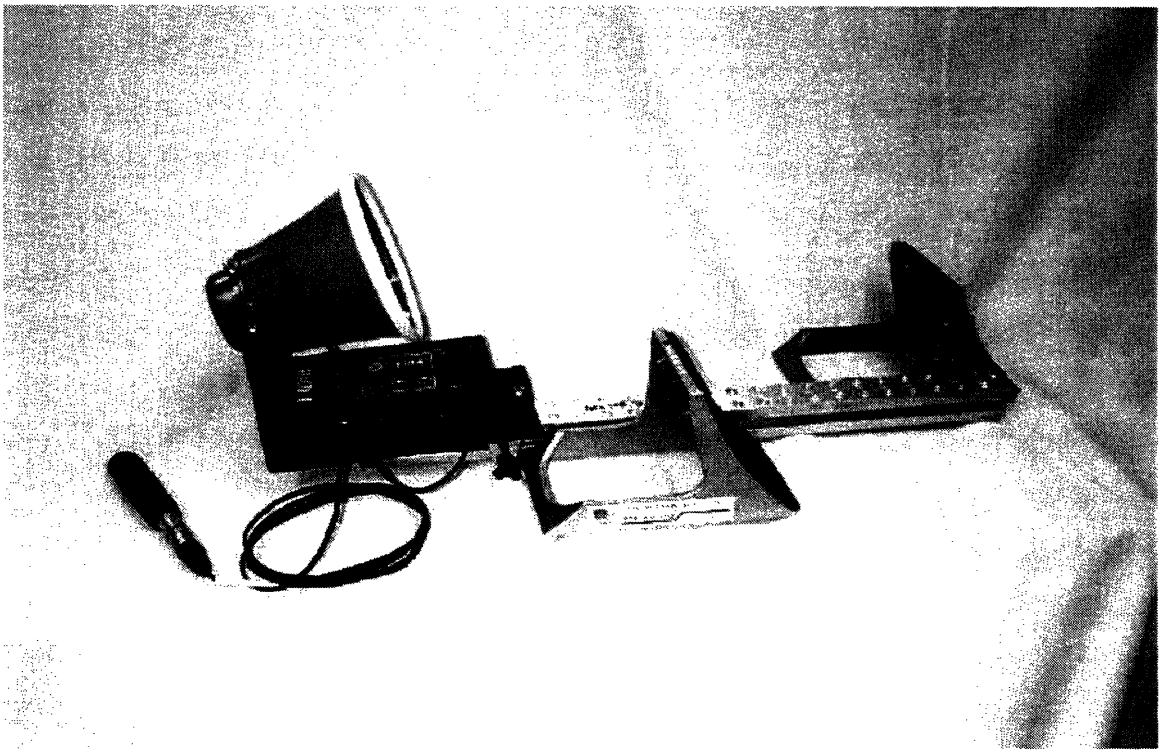

Figure 1: *FinishLynx Inc ReacTime starting blocks. The unit employs an accelerometer that attaches to the rear of the blocks. The laptop and connecting cables needed to run the unit are not shown.*

1.3 Goals

This system takes a fundamentally new approach to measuring the forces of an athlete's start by imbedding a flexure within each foot pad. This system is able to measure forces directly and in concrete units instead of inferring abstract force measurements from forces that propagate through the blocks. The embedded measurement system is capable of recording forces in several directions in addition to the horizontal, and is further able to deduce the location of the center of force during push off, giving more comprehensive and more complete data about each start. Wireless supporting electronics do away with the long and complicated set-up time and make this set-up a fully portable and easily deployable starting solution.

1.4 Overview

Chapter 2 gives a high level description of the solution and describes the product architecture and the major interfaces. This chapter also covers the detailed design of each module and gives the supporting theory behind each design choice.

Chapter 3 discusses the calibration procedure and the determination of experimental constants predicted by theory. The calibration results are displayed an analyzed later in the chapter.

Chapter 4 details the field testing procedure and collection of actual starting data. The analysis and numerical synthesis of the starting mechanics of a collegiate athlete are included in this section.

Chapter 5 discusses opportunities for further research, including further testing that could be performed with this apparatus as well as possible alternative designs suggestions for moving forward with the current implementation.

Solution Design

From concept to final implementation, customer needs have guided the design process. The final iteration employs a stiff flexure embedded within each footpad to satisfy the need for a rigid measurement system that does not deflect during the start. Additional modules ensure that the unit is robust and durable enough to withstand environmental effects and the regular abuse of being dropped, stored, and punished during an average track workout. The entire unit is also designed to be cost effective to manufacture, as customer needs dictate that the entire unit cost less than $500 to manufacture. The modified blocks retain the best features of adjustability and portability that exist in regular mechanical blocks.

2.1 Product Architecture

The design consists of four major subassemblies: the *footplate*, the interface that contacts the runner's shoe, the *adjustment plate* which supports the foot plate and adjusts its angle with respect to the ground, the *enclosure* assembly which protects the electronics and the transducer, and the *transducer* itself, which measures the imparted forces.

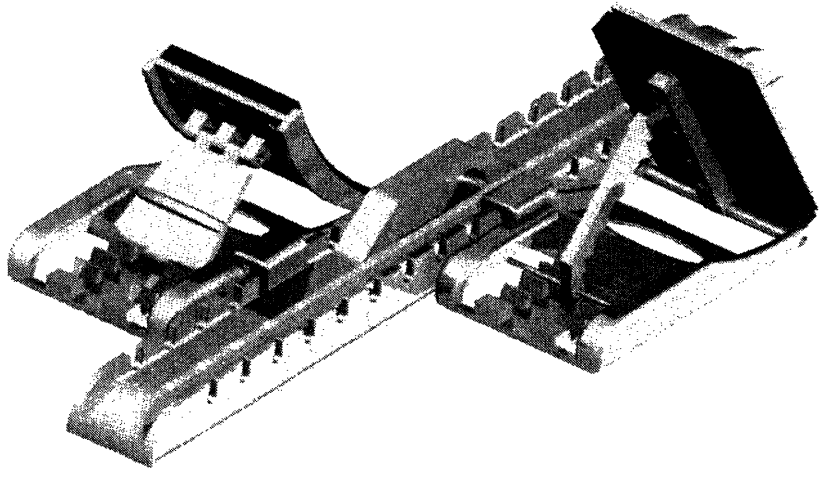

Figure 2: *Modified track blocks displaying the original footpad at left and the enhanced footpad at the right. The center rail positions the footpads with respect to one another.*

2.1.1 Foot Plate

The footplate is the only part of the blocks that touches the athlete during the race, so the perceived quality of the blocks during the actual start is determined solely by this piece. Though for ease of manufacturing, the prototype footplate is a flat piece, the production part could be slightly curved for improved ergonomics. Additionally, the production part would have a rubberized front surface to accommodate spikes and to prevent slippage.

The prototype piece itself is made from honeycomb aluminum to provide stiffness at low weight, though the production piece could be cast.

2.1.2 Enclosure

The enclosure prevents the hostile environment from damaging the fragile components of the transducer. The enclosure is simply a drawn sheet metal box that attaches to the adjustment assembly to surround the flexure. A thin, compliant rubber membrane extends to the back face of the footplate to keep dirt, dust and grime from getting near the circuitry or other inner components. Additionally, the enclosure defends against large objects such as spikes or batons that could dislodge wires or disrupt gages. The back of enclosure accommodates the electronics interface that connects the transducer to the central processor at the rear of the blocks.

2.1.3 Adjustment Assembly Design

The adjustment assembly supports both the transducer and enclosure and adjusts them to different angles with respect to the ground. The angle of the blocks can be adjusted by lifting the handle portion of the assembly and placing its base in a series of notches. The

finger grooves on the handle both increase ergonomics and give the user some visual information about how the assembly is supposed to be used.

When the handle is removed from the assembly, the remaining piece can be used as a test-bed to calibrate and zero the transducer. The test-bed has two 6mm through holes that allow the entire footpad to be mounted securely on a standard bench top.

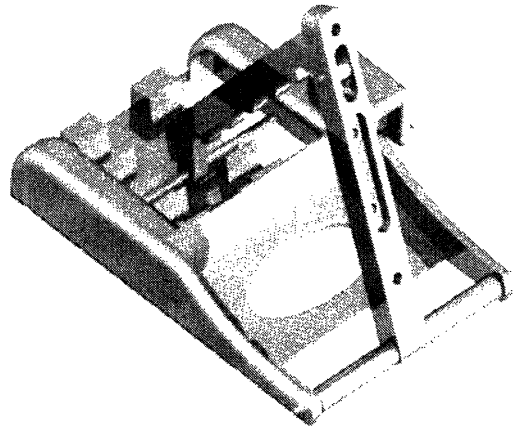

Figure 3: *Adjustment assembly*

2.2 Transducer Design

2.2.1 Mechanical Design

After several iterations, the design of the transducer settled on bending beams for their sensitivity to light loads, specifically forces less than 400 lbs. Typical axial force transducers are designed to accommodate loads upwards of thousands of pounds. Modifying these existing designs to take light loads would have meant thinning down some sections so small that they would perform well in tension but buckle under any compressive or side load. Bending beams have the advantage of being relatively large (on the order of .5 inch thick) while still being able to produce large strains in response to loading by concentrating stress in the outmost fibers of the beam.

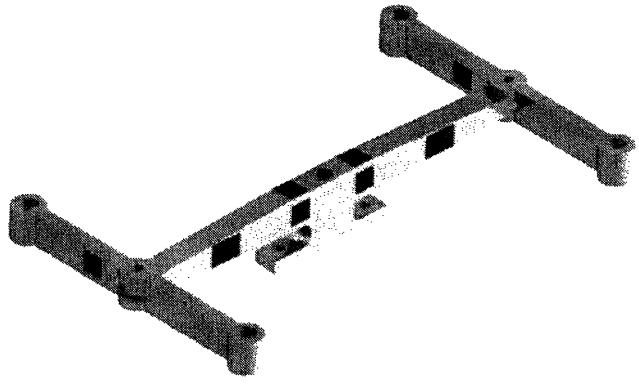

Figure 4: *Force transducer. The darker patches are mounted strain gages.*

For this design it is assumed that the runner cannot impart moments on the footpad, since his feet do not adhere to the blocks and he could not "pull" on any part of them. It is possible that the foot could twist about the lower leg, but this moment would be small compared to the forces imparted along the other axes, and for the purpose of this thesis is not considered a significant source of wasted energy. Thus the transducer focuses on capturing the time variation of just five data sets for each start: the compressive load directed normal to the footpad, the side load directed horizontally outwards from or inwards to the blocks, the end load directed vertically down towards or up from the track, and the vertical and horizontal positions of the net load on the footpad surface.

The two center spans are responsible for detecting the magnitude of the compressive and horizontal loads as well as the position of the center of force. Because these beams are insensitive to axial loads, additional beams are mounted at the end of each center span in order to register the end loads with better accuracy. Predictions of applied loading were taken from a study of starting mechanics done by Halston Taylor, coach of the MIT track team, in 1995. In his study the heaviest compressive load by an athlete during a start was 150 kg, ranging down to 70 kg for lighter and weaker athletes. Thus the design is tuned to this range of forces with the ability to withstand forces upwards of 200 kg and the sensitivity to detect loading to within 1 kg anywhere in the range from 0-200kg. The transducer is tuned for off axis loads approximately 10% of those in compression, though the transducer could withstand and accurately measure forces up to 50% of the compressive load before risking plastic deformation.

2.2.1.1 Important Factors in Force Transducers

The center spans are essentially cantilever beams undergoing simultaneous loading in all three directions in addition to axial torque. Fortunately, clever placement and arrangement of measurementation can separate out the effects of the different loads, so a single member can be used to measure several parameters. Isolating and measuring strain in a single direction is fairly straightforward. The challenging aspect of the transducer

design is in generating these strains in a predictable and practical way. The designer must ensure that:

A) The applied load generates enough strain to be accurately measured but not so much as to induce plastic deformation in any part of the transducer
B) Each of the applied loads (normal, horizontal, and vertical) incurs strains of the same order of magnitude
C) Each of the applied loads generates strain that is linearly related to its magnitude
D) Manufacturing and assembly of the transducer is mechanically possible and economically feasible
E) Application and assembly of measurement instrumentation is physically possible and economically feasible

Many commercial transducers attempt to cancel out side loads and thus the transducer is stiff in every direction except the one to be measured. In contrast, this design seeks to capture both the axial loads and the end and side loads, so it must be compliant enough in every direction to generate measurable strains while being stiff enough not to plastically deform or buckle.

2.2.1.2 The Precision Elastic Limit

The acceptable limit of strain is known as the Precision Elastic Limit, (PEL), defined as the stress level that will cause a permanent elongation of one millionth of a cm per cm. The yield stress Y is the stress threshold that induces 0.2 % plastic, or permanent, deformation. Of course, the transducer could not deliver reliable data if every cycle induced .2% plastic strain, because these small deformations would quickly add to create permanent aberrations in the beams. In theory, all metals are completely elastic in reaction to loads less than the yield stress. In reality, however, even small stresses produce some tiny plastic deformations. In practice the transducer can be considered undeformed only if the loading generates strain less than the PEL. Data on the exact PEL

stress for 6061 T6 Aluminum is scarce, but a safe estimation is approximately 100 MPA, less than 1/2 the yield stress of 240 MPA.

2.2.1.3 Bending Beam Theory

So long as no stresses exceed the precision elastic limit, the first of the five challenges of the transducer design is satisfied. The second criterion of tuning the sensitivities is accomplished by exploiting mechanics of materials. The vertical load is measured by a dedicated beam. This allows great flexibility in engineering, as this beam is not constrained by the geometry requirements imposed on the multifunctional center beams. The end beam needs only reflect the one load while canceling the others. The center span on the other hand measures two perpendicular loads and a torque simultaneously, so its geometry is tightly constrained. The stresses in the center span are governed by well known bending beam theory. For a beam fixed at one end and loaded at the other, the moment in the beam as a function of its length is

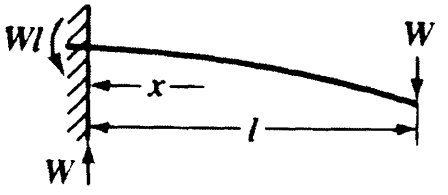

Figure 5: *Free body diagram of a cantilever beam fixed at one end and loaded at the other.*

$$M = \frac{W}{(l - x)} \qquad \textit{(Equation 1)}$$

Where l is the length of the beam, x is the distance from the fixed end, and W is the load applied at the free end. Thus the moment is greatest at the fixed support, and the internal stress is greatest in the top and bottom fibers. The internal stress in the beam under elastic loading is depicted as shown:

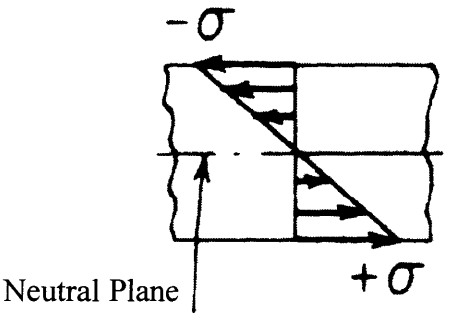

Figure 6: *Internal stress distribution of the cantilever beam before undergoing plastic deformation. The strain is greatest in the uppermost and bottommost fibers.*

With the maximum stress occurring in the fibers furthest from the center axis of bending. For these fibers this stress σ is equivalent to

$$\sigma = \frac{Mc}{I} \qquad (2)$$

Where M is the applied moment, c is the height from the bending axis, and I is the moment of inertia of the cross section. These are the three major variables that can be changed in order to alter the maximum stress, and therefore the sensitivity to each of the applied loads.

The moment on the beam can be decreased by a factor of two if the free end is instead guided. For a cantilever beam fixed at one end and guided on the other, the stress at any point is described as,

$$M = \frac{W}{2(l-x)} \qquad (3)$$

So again the moment is greatest at the extremities with magnitude equal to only half that of the free beam.

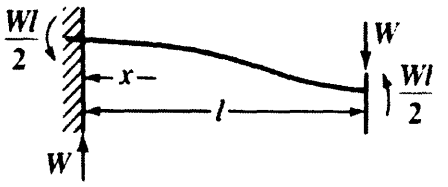

Figure 7: *Free body diagram of a cantilever beam fixed at one end and guided and loaded at the other.*

The moment of inertia can also be altered to favor bending in one direction more than the other. Because the beam is rectangular in cross section, it is naturally stiffer in response to compressive loads and more compliant in response to side loads. For a simple rectangle the moment of inertia varies linearly with width *b* and as the cube of the height *d*:

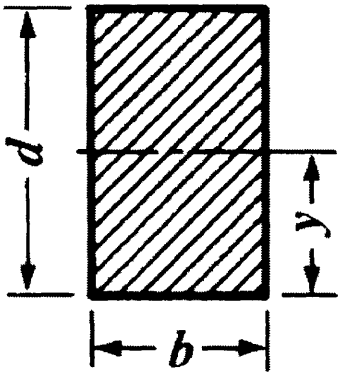

Figure 8: *Cross section of a rectangular beam.*

$$I = \frac{bd^3}{12} \qquad (4)$$

if *y* denotes the bending axis. The center spans are 3/8" thick and 1/2" thick at their junction with the central support. Thus, in the direction of the compressive load, the moment of inertia is:

$$I_{compression} = .\frac{375in * .5in^3}{12} = 1.625 * 10^{-9} m^4 \qquad (5)$$

And in the direction of the horizontal load,

$$I_{horizontal} = .\frac{.5in * .375in^3}{12} = 9.1457 * 10^{-10} m^4 \qquad (6)$$

Once again a factor of two difference, combined with the factor of two difference contributed by the different end conditions, artificially inflates the side load to four times greater than for an non-optimized square beam. The end beam is easily optimized because its only constraint is the PEL. It is therefore stiff in the direction of compressive loads and compliant in the direction of vertical loads, with maximum stress tuned to be almost the same as the expected stress in the center span due to horizontal loads. The maximum stresses in responses to compression, S_{comp}, horizontal load S_{side}, and vertical load S_{end} are:

$S_{comp} = 9.3000 * 10^7$ Pa

$S_{side} = 2.4800 * 10^7$ Pa

$S_{end} = 2.6156 * 10^7$ Pa

The final measurement to be taken on the center span is torque. The torque applied at the end of the beam incurs a shear stress that is linearly proportional to the torsional moment of inertia at every point along the beam's length. Tuning the beam's sensitivity to torque is thus a simple matter of altering this moment of inertia. This is accomplished with a gentle taper along the beam's length. The measurementation can then be placed anywhere along the length to register the desired strain. In this case, the measurementation is placed at the point of greatest stress concentration allowed by geometric constraints. This gives

$S_{shear} = 7.4125 * 10^7$ Pa

Which is of the same order of magnitude as the other measured stresses.

The only one of the three variables determining maximum stress that was unchanged was the distance from the bending axis, *c*. It is unlikely that this parameter would be optimized, since changing this parameter only alters the measured stress, not the maximum stress imparted.

Note from Equations (1) and (3) earlier that the use of cantilever beams guarantees a linear relationship between the applied load and the incurred stress. This satisfies the criterion that the transducer linearly convert load to strain.

The final step of the design is to verify that the transducer as designed can be feasibly manufactured and assembled, and that the instrumentation can be applied in the correct position and orientation. The center span is of uniform thickness and easily cut from .375" aluminum sheet stock. Likewise the end beams can be cut from .50" aluminum sheet stock and post-machined with little overhead lost to tool changes and fixturing. The dimensions of each piece are more than large enough to accommodate strain gages as a measurement tool. These pieces are therefore inexpensive to manufacture as required.

2.2.2 Measurementation Design

Strain gages are used on the flexure to precisely measure the strain of each part of each member. Strain gages are long, low resistance wires that exhibit a change in resistance under mechanical strain. The wire is packaged into a small space and mounted on a flexible backing that can be bonded to the surface to be measured. At the surface strains, so does the wire, changing its resistance by a very small amount. Special circuitry can be used to convert this small change in resistance to a readable change in voltage that can be measured hundreds of times per second by computer.

2.2.2.1 Strain Gage Characteristics

Strain gages make sense as a measurement tool because they are very small, essentially only the thickness of the wire and less than 1/3" square. Provided that the mounting

surface is accessible, they can be mounted almost anywhere, including curved surfaces. At the very least, the transducer must measure 5 parameters: the three major forces and two positions, so if a separate measurement system is to be used for each measurement then it must be very small and easily mounted.

Strain gages also run on low power, a critical requirement for a portable, battery powered device such as this one. The circuitry associated with the gage runs on 5V and draws fewer than 10 mA, with no theoretical lower limit on either voltage or current. If the circuitry downstream of the gage could be shielded from electrical interference, the gage could run on arbitrarily low power.

Additionally, strain gages are appropriate for both static and dynamic measurement and respond instantly since they are mechanically connected to the surface they measure. This allows them to accurately measure strains at frequencies far in excess of 100 Hz.

Finally, strain gages naturally integrate the strain over the area on which they are applied. This naturally helps to reduce irregularities caused by the fact that the aluminum is not a perfect crystal as theory supposes. Integration over an area helps to reduce local strains caused by nicks and scratches in the surface, and also combats bulk defects like uneven heat treatment.

Though flexible and relatively inexpensive, strain gages are prone to several problems that must be minimized through design choices:

Linearity, hysteresis, and zero shift are interrelated functions that arise from the interface between the substrate material, the bonding adhesive, the strain sensitive material and the gage backing material. Fortunately all of these factors can be controlled except for the substrate material, and deviation from linearity can be kept less than .1%. Similarly hysteresis and zero shift can be kept below .2% of the maximum strain. For this application the gage backing and strain sensitive material are both selected to match the Aluminum mounting surface.

Drift is a time dependent and generally irreversible change in resistance due to varying temperatures under no mechanical load. This is an issue for the transducer as it is likely to see a wide temperature range during its lifespan, indoors, outdoors, and during transit. Modern gages show strain of just a few in a million parts per year, so this effect could be minimized in software by zeroing the blocks before use. Because drift increases with temperature, the effect can be minimized by storing the blocks in a cool area. The enclosure will prevent direct heating by sunlight.

Creep, unlike drift, is the time dependent and irreversible change in resistance under mechanical load and at constant temperature. Care must therefore be taken to store the entire unit in an unloaded configuration: i.e. on a rack instead of stacked one on top of the another. Creep during the actual start can be neglected, as the blocks are only loaded for less than a ¼ second for each start. The total time under load while starting is miniscule compared to the lifespan of the blocks (and the athlete).

Because the surface being measured is part of a large member, heat dissipation is not a problem in this application. Although several gages are simultaneously operating at 2-6 mA, the thermal mass and surface area of the Aluminum substrate make it an effective heat sink, and temperature effects can be neglected.

2.2.2.2 Strain Gage Selection

Some care must be taken to choose the correct strain gage for a given application. The gages selected are the Vishay Micro-Measurement dual linear transducer class strain gage model N2A-13-S138K-350 and Omega Precision Dual Shear strain gage model SG-6/350-TY43. These particular models were selected based on several critia:

Wire length contributes to the gage's sensitivity to strain. Thus, the longer the gage length, the greater the change in resistance for a given stress. The gage length was chosen to be the greatest possible while still fitting within the geometric constraints of the

beam. Also, as stated earlier, integration over the area of the gage is a desirable effect, and longer gage lengths are directly linked to large coverage area.

Several *patterns of gages* exist although this application employs dual linear gages to guarantee that certain gages are parallel to one another. A single dual linear gage contains two gages mounted on the same backing, so alignment is performed during manufacturing rather than during mounting. For torque measurement the shear gages are also packaged on the same backing to ensure that they are mounted at the correct angle with respect to one another.

In general the *gage resistance* is chosen to be as high as possible to reject ambient noise. Very low resistance gages promote lead wires to act as antennae for unwanted signals, and recovering the signal from the background noise can be difficult because the signal is very small. Here the only limiting factor was cost, as price varies almost exponentially with resistance. Thus the gages at 350 Ohms are slightly more resistant than more common 120 Ohm gages, though not nearly as strong as the available 1K and 5K Ohm variety. Higher resistance gages also reduce heat dissipation, though as earlier stated this is not a serious problem.

The *strain sensitivity* of a strain gage, G_f, is a dimensionless proportionality factor between the relative change in resistance ΔR and the strain to be measured ε:

$$\frac{\Delta R}{R} = G_f \varepsilon \qquad (7)$$

so of course it is desirable to have this number be as high as possible. For the gages selected here, the gage factor is just above 2 at room temperature. Transverse sensitivity is a measure of the gage's response to off-axis strain, so likewise it is desirable to have this number be as small as possible. Both the gage factor and the transverse sensitivity are determined by measurement of sample gages for a given production run, so there is

some small variance among the batch. This is a potential source of error that can hopefully be reduced by using more than one active gage in each measurement circuit.

2.2.2.3 Strain Gage Assembly Concerns

Inaccuracies in strain gage mounting will lead to small loss of sensitivity in the primary direction and will lead to increased sensitivity to off-axis loading. However, one of the major strengths of this design is that it can be calibrated after construction, so all of the inaccuracies in assembly and manufacturing can be essentially nullified before use. The user can nullify the errors due to zero shift, creep and drift in software simply by zeroing the blocks before each use. Similarly if they have a known weight, they could reset the blocks' sensitivity to loading. The design must guarantee that the applied loads generate large measurable strains in a linear fashion, and must predict that errors and variations be small. However, theory does not need to predict all of the inevitable errors in measurement because most of them will be accounted for during calibration.

2.2.3 Circuitry Design

2.2.3.1 Introduction to the Wheatstone Bridge

Circuitry within the footpad employs full wave Wheatstone bridges to detect the very slight changes in resistance in the strain gages. The bridge is being used as an *unbalanced system;* the bridge output is directly connected to a voltage measurement device that samples at a constant rate. This system has the advantage of handling static and dynamic loading equally well, but requires a stable and reliable power source. This source is provided by an LM7805 power source and several Operational Amplifiers serving as voltage followers. The bridge is only powered for the duration of the start, so the voltage source does not need to stay active for longer than a second at a time.

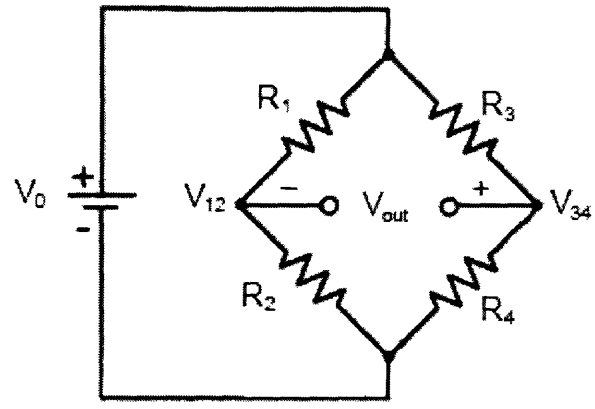

Figure 9: *Wheatstone bridge circuit diagram. Note that in the field, V_0 is provided by a LM7805 power source using operational amplifiers as voltage followers.*

The use of four arm Wheatstone bridges offers several advantages over double- or single-arm bridges. Most importantly the four gage bridge on the bending beam naturally cancels out unwanted side loads and moments. This is critical in this application as one beam is being forced and torqued in several directions at the same time. The four gage bridge is also automatically compensated to reject common mode noise such as temperature variation. In a single arm bridge, temperature change would be indistinguishable from strain. In this case, so long as all four gages are the same temperature, heating and cooling will not affect the bridge output. Finally, the voltage output of the four gage bridge is 4 times greater than the single arm, making the signal stronger in comparison to background noise and providing added sensitivity to strain.

If the bridge is initially balanced and idealized conditions are assumed, the voltage output from the bridge can be expressed as:

$$V_{out} = \frac{V_0}{4R_0}\left[\Delta R_1 - \Delta R_2 - \Delta R_3 + \Delta R_4\right](n-1) \qquad (8)$$

where n is a nonlinearity factor, R_0 is the unstrained resistance of each of the four gages in the bridge, and R_1, R_2, R_3, and R_4 are the resistances of the gages under mechanical

strain. In the case where two gages each are placed on opposite sides of the bending beam, the nonlinearity factor drops out giving the bridge output voltage V_0 as a direct linear relationship in terms of strain ε and the gage factor F_g:

$$V_{out} = \left(\frac{\Delta R}{R_0}\right)V_0 = F_g \varepsilon V_0 \qquad (9)$$

Each bridge is adjustable by a variable resistor placed in parallel with one of the strain gages. This allows for fine tune adjustment to compensate for the slight tolerance in the strain gages as well as interfering resistance in the connecting wires. The zeroed bridge output can then be amplified and filtered before being fed into an A/D converter. The wiring diagram of the modified bridge is shown below.

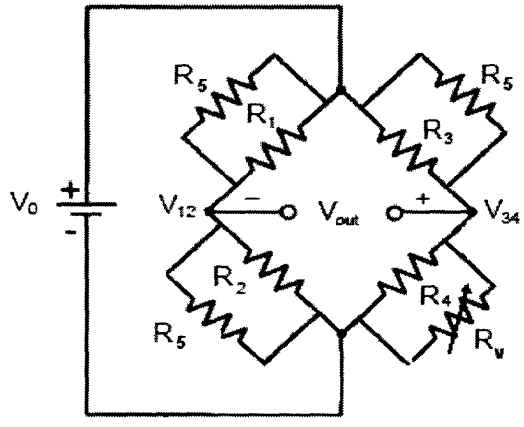

Figure 10: *Modified Wheatstone bridge circuit, with large resistors (5K Ohm) placed in parallel with the active arms R_1, R_2, R_3, and R_4 of the bridge. R_v is a variable 10KOhm resistor used to balance the bridge.*

2.2.3.2. Gage Arrangement

Consider one of the two beams in the center span The beam is loaded in three directions and torqued as shown below:

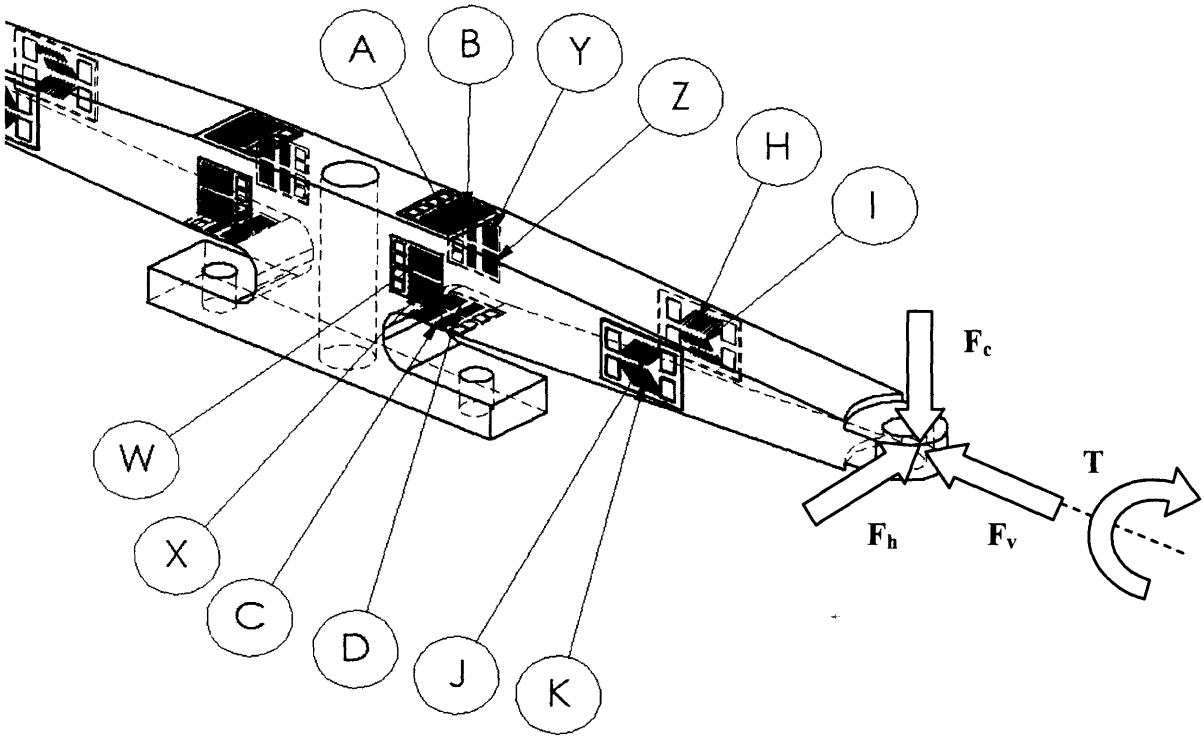

Figure 11: *Placement of strain gages on one member of the center span. The applied loads on the beam are F_c, the compression force, F_v, the vertical load, and F_h, the side load. A torque T acts about the long axis of the beam.*

with strain gages placed diametrically opposed to each other to capture the strains incurred by each load. In the diagram above, the strain gages A B C, and D capture the strains due to the compression force F_c, the gages marked W, X, Y and Z capture strains due to the side-load F_h, and the shear gages marked H, I, J and K capture the shear strains incurred by the torque T. The gages are arranged in bridges as shown below:

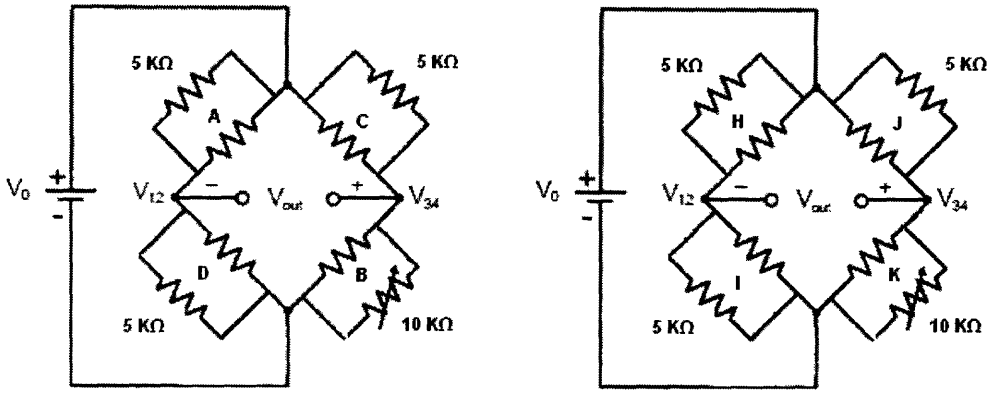

Figure 12: *Arrangement of strain gages into Wheatstone bridges. All the bridges employing linear gages are similar to the diagram at left. The two torque bridges are arranged as shown at right.*

This arrangement naturally minimizes crosstalk between bridges.

2.2.3 Transducer Output Interpretation

As dictated in section 2.2 Transducer Design, the voltage output of the Wheatstone bridge in response to F_c is linear. An ideal relationship between the output voltage and the compression force would therefore be:

(10)

$$F_{c_1} = \frac{V_i}{K_i}$$

where V_i is the voltage output from the bridge, and K*i* is a constant. Though F_h and T should be completely independent of the voltage output, realistically there is some dependency due to alignment error of the gages. If one of the dual linear strain gage pairs is mounted off center, then it will respond slightly to perpendicular loading. If the gage is mounted on center, but tilted, it will respond to shear forces. Therefore a realistic statement of equality between the actual compression force and the voltage output of the corresponding bridge is:

(11)

$$F_{c_1} = \frac{V_1}{K_1} + c_1 F_{h_1} + c_2 F_{v_1} + c_3 T_1$$

where c_1, c_2, and c_3 represent the sensitivity of the compression measurementation to off axis loading of beam 1. Only the axial toque is counted here, since beam is free to rotate about the pinned end. Because of geometric constraints imposed by the footplate, the radial torque is completely dependent and does not need to be included as an independent variable. The same equations are true of beam 2 in the center span, giving the following equation for the total compression force on the footplate:

$$F_{c_1} + F_{c_2} = F_c = \frac{V_1}{K_1} + \frac{V_2}{K_2} + c_1 F_{h_1} + c_4 F_{h_2} + c_2 F_{v_1} + c_5 F_{v_2} + c_3 T_1 + c_6 T_2 \qquad (12)$$

By observation, the sensitivity terms c_2 and c_5 corresponding to the axial loading F_v drop out immediately. The strain due to axial loading is negligible compared to bending, and is further more rejected as common mode noise by the Wheatstone bridge. Also, if it is assumed that the gages are mounted reliably and symmetrically, the sensitivities for opposite sides of the transducer should be approximately equal. This leaves the simpler equation:

$$F_c = K_1(V_1 + V_2) + c_1(F_{h_1} + F_{h_2}) + c_2(T_1 + T_2) \qquad (13)$$

Using similar logic produces the corollary equations expressing the torque T and side load F_h:

$$T = K_2(S_1 + S_2) + c_3(F_{c_1} + F_{c_2}) + c_4(F_{v_1} + F_{v_2}) \qquad (14)$$

(15)

$$F_h = K_3(H_1 + H_2) + c_3(F_{c_1} + F_{c_2}) + c_4(T_1 + T_2)$$

since again the sensitivity of F_h to axial loading is negligible. On the outer beams, the loading is as depicted below:

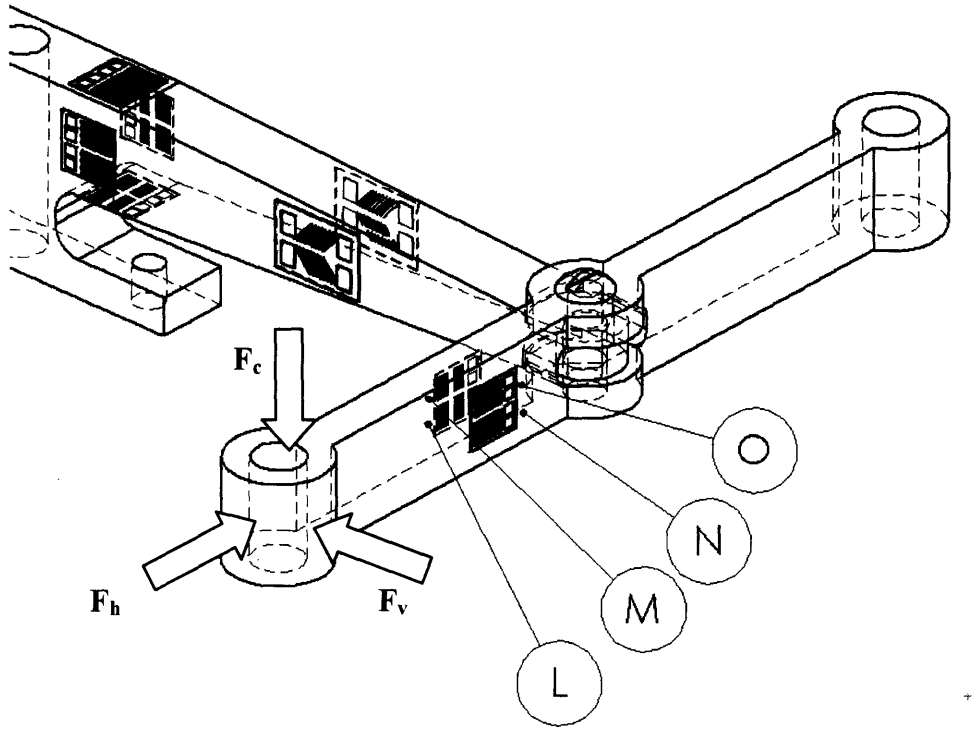

Figure 13 *Placement of strain gages on one member of an outer beam. Again, the applied loads on the beam are F_c, the compression force, F_v, the vertical load, and F_h, the side load. Note that the magnitude of each load is less than in the previous diagram since the load is distributed over two more beams.*

As long as the footplate is rigid and remains flush with the top of the beam, and the beam is free to rotate about its pinned end, there can be no applied torques. Again, axial loading can be neglected. Therefore the output voltage E_i from the strain gages on outer beam *i* is a linear function of the vertical force F_{vi} and disturbances from the compression force F_{ci}:

$$F_{v_i} = \frac{E_i}{K_i} + c_i F_{c_i} \tag{16}$$

and because there are four beams symmetrically constructed and assembled:

$$F_v = K_4(E_1 + E_2 + E_3 + E_4) + c_5(F_{c_3} + F_{c_4} + F_{c_5} + F_{c_6}) \tag{17}$$

The position Y of the center of force from the vertical midline is calculated directly from the measurements of F_{c1} and F_{c2}:

$$Y = l\left(\frac{F_{c_1}}{F_{c_1} + F_{c_2}} + 1/2\right) \tag{18}$$

where l is the vertical length of the beam. Equations 13, 14, 15, and 17 can be reduced to a single matrix:

$$\begin{bmatrix} \sum V \\ \sum E \\ \sum H \\ \sum S \end{bmatrix} = \begin{bmatrix} c_1 & k_1 & 0 & c_2 \\ 0 & c_3 & k_3 & c_4 \\ k_2 & c_5 & 0 & 0 \\ 0 & c_6 & c_7 & k_4 \end{bmatrix} \begin{bmatrix} F_h \\ F_c \\ F_v \\ T \end{bmatrix} \tag{19}$$

$$\sum V = [M]F \tag{20}$$

Testing in Section 3 will determine values for each of the constants c_i and K_i in each of the above equations.

Transducer Calibration

3.1 Calibration Set-up and Procedure

As stated in section 2.2.2.3 Strain Gage Assembly Concerns, testing of the prototype only has to verify sensitivity and linearity of the transducer in response to loading. Each of the sensitivity terms k_i and c_i in Equation (19) were determined by loading the transducer with a set of known masses.

The Wheatstone bridges were constructed on breadboard using high tolerance resistors and 20 turn screw-type 10K pots. An HP 3610A power supply was used to provide a steady floating 5V signal over the bridge, and the output was read with an HP 973 A Digital MultiMeter (DMM). The DMM was accurate enough to measure millivolts to two decimal places, and was used in rolling average mode to decrease high frequency background noise.

Each set of strain gages was then connected with mini-clips to the Wheatstone bridge via short, shielded coaxial cables. For every gage set in the center span, the corresponding member was loaded in the three major directions up to 20 lbs in 5 pound increments, with several measurements taken for each loading condition. The beam was also torqued up to 40 inch-lbs in both directions. The results of this testing are discussed in Section 3.2.

3.2 Calibration Data and Results

The results of a sample calibration are shown in Figure 14.

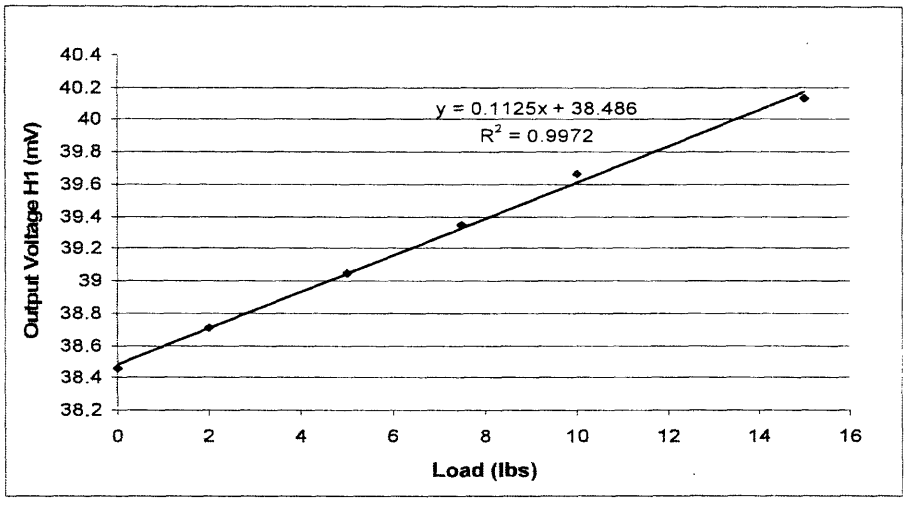

Figure 14: *Unamplified voltage output from a Wheatstone bridge in response to loading.*

Here the slight DC offset (~38.5 mV) is a result of slight imbalance in the Wheatstone bridge prior to loading. Though completely eliminating the DC offset is not necessary, allowing the DC offset to grow too high could cause non-linearities in the output curve. The sensitivity k_2, corresponding to the output voltage H_1 in response to horizontal loading, is equal to the slope of the graph, .1125 millivolts per pound.

This single test validates several parts of the theory, most noticeably that the response is shockingly linear. Further testing up to the expected load of 15 kg (~35 lbs) shows the same linearity with a variance (R^2 value) of .992. This test also demonstrates sensitivity that is of the same order of magnitude as was predicted by theory.

Filling in the results of each of the other tests gives the matrix in its numerical form:

$$\begin{bmatrix} \sum V \\ \sum E \\ \sum H \\ \sum S \end{bmatrix} = \begin{bmatrix} 0 & .035 & 0 & 0 \\ 0 & -.001 & .039 & 0 \\ .112 & 0 & .004 & 0 \\ -.002 & .005 & 0 & .097 \end{bmatrix} \begin{bmatrix} F_h \\ F_c \\ F_v \\ T \end{bmatrix} \qquad (21)$$

Constants less than .001 are listed as zero. For testing in the field, this matrix is inverted to derive the applied forces from the measured voltages:

$$\begin{bmatrix} -.026 & -.9158 & 8.929 & 0 \\ 28.571 & 0 & 0 & 0 \\ .732 & 25.641 & 0 & 0 \\ -1.473 & -.019 & .184 & 10.309 \end{bmatrix} \begin{bmatrix} \sum V \\ \sum E \\ \sum H \\ \sum S \end{bmatrix} = \begin{bmatrix} F_h \\ F_c \\ F_v \\ T \end{bmatrix} \qquad (22)$$

Field Testing

The purpose of the field testing was both to test the flexure's performance in real time and to gather data about an actual start. Because the onboard processor that will capture data is not yet complete, the information generated by the transducer was collected two inputs at a time by a personal computer. For the testing in the following sections, these two inputs are the most critical in the entire design: the measurements of the compressive loads on each of the two center spans.

4.1 Field Setup and Procedure

For the field test the flexure was assembled into the footpad and an actual athlete performed several starts in the lab to simulate a race on the track. Because the expected output data was some type of waveform, to capture dynamic data the DMM was replaced by a desktop PC.

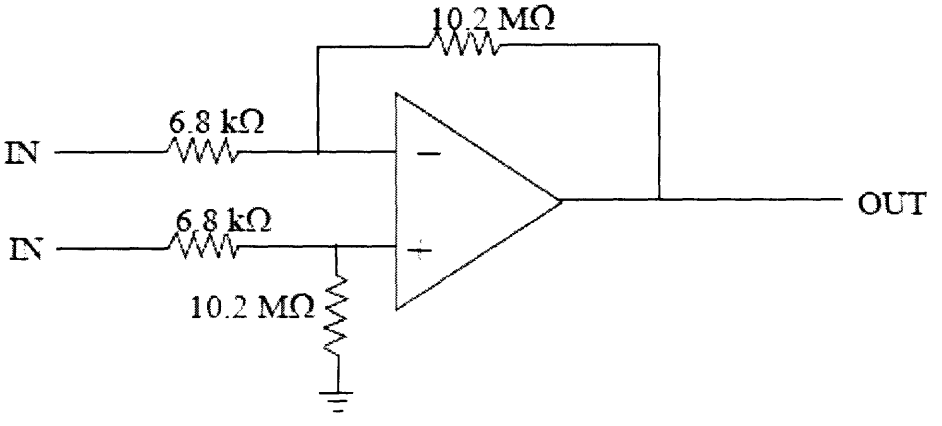

Figure 15: *Differential Amplifier circuitry*

A desktop PC was used to record data in real time, so the raw signal from the Wheatstone bridge had to be amplified from its typical range of ~1 mV via a differential amplifier. The long lead wires leading to the strain gages act as antennae for unwanted noise, so the

differential amplifier was placed close to the footpad in order to preserve the signal. At the center of the amplifier is a 277 Operation Amplifier supplied by +/- 15V. This voltage range is clearly not suitable for final production since batteries cannot supply this range effectively. However, for verification of the mechanical design this setup was cost effective and easy to construct. The gain provided by the amplifier produced voltage outputs on the order of 1V, nearly 1000 times greater than the raw signal, with no noticeable noise. The amplified signal was fed into the parallel port on the PC. For these tests the data was sampled at 200 Hz, twice the speed projected for use in the field.

With the circuitry in place, the footpad was mounted to the bench top with the footpad facing the ceiling. Each beam was then calibrated independently using a spring scale and several large weights. The spring scale was placed at several points on the vertical and horizontal axes of the footpad, and at each point loads were applied up to 20lbs in 5 pound increments. Data was read in at 10 Hz during the loading process to take several measurements at each load, hopefully eliminating errors due to misalignment of the spring gage. Among the points tested were the positions directly above the ends of each center beam where they connect to the outer members. This data, discussed in 4.2.1 Field Calibration, was used to verify that the output voltage of the transducer varied linearly with the vertical position and the magnitude of the applied loads.

To test the footpad's response to heavy loads, two large training weights weighing 35 and 45 pounds were placed on the flexure, and the 20lbs of the spring scale were added on top to give a total load of 100 pounds.

For the actual test, the block was placed on the ground and lodged against the base of the wall. The athlete then took several starts exactly as he would have in the field. At a collegiate level, this means a "3 command start". On the first command, "*On your marks*", the athlete puts his feet on the blocks and his hands behind the starting line and stays motionless until the next command. On the second command, "*Set*", the runner lifts his torso and shifts the majority of his weight to his hands, raising his hips and flexing at the knees. On the third command, the gun, the race starts and the runner pushes out of

the blocks. The blocks are set up with one footpad in front of the other, with the front leg responsible for most of the push off force. Therefore the front footpad of the block was replaced with the modified transducer footpad.

Due to space constraints the athlete was not able to accelerate to full speed, but the first few steps were very representative of an actual start. The compression force on each of the center members was sampled at 200Hz for each trial, where the athlete was told to vary his foot placement and start intensity. Trials 1, 2, and 3 measured the response of just once beam at a time. Trials 4, 5, and 6 recorded data from both beams simultaneously.

4.2 Field Test Results

4.2.1 Field Calibration

The results of the calibration are shown below. Figure 16 is the loading profile for just one of the many points that were tested for each beam. The five plateaus correspond to the 0, 5, 10, 15 and 20 pound applied loads. To develop a correlation between the applied load and the output voltage, the plateaus were averaged and plotted to test for linearity. The plot of all the loadings at various vertical positions is shown in Figure 17.

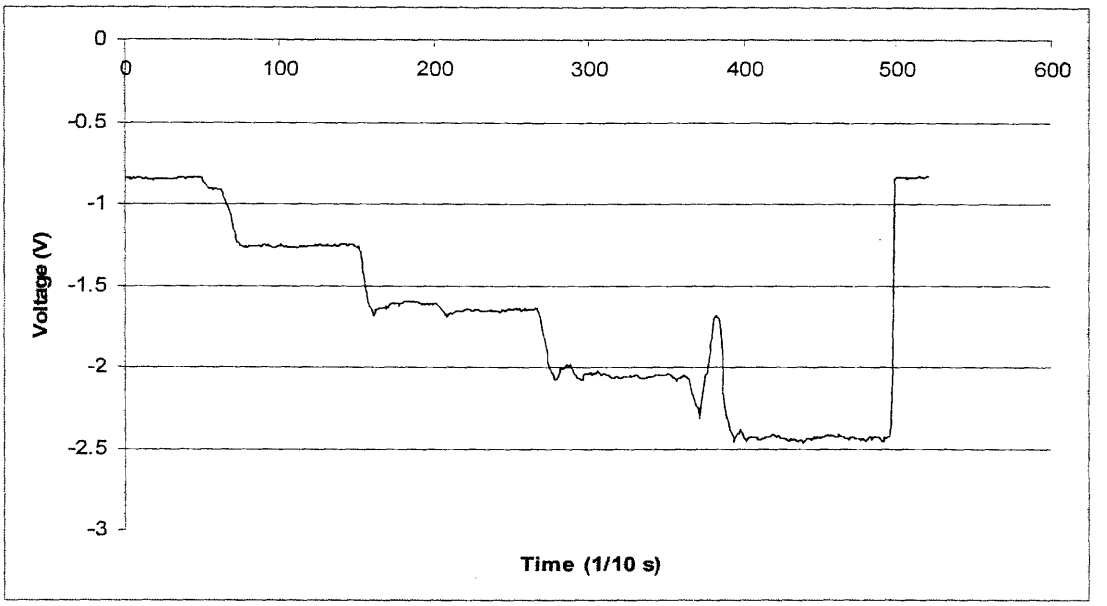

Figure 16: *A sample field calibration where the load on the foot plate was varied in 5 pound increments and sampled in real time. For this trial the load was centered horizontally and vertically spaced 1.75 inches above the center axis.*

Each of the lines below is a best linear fit of the voltage output vs. the applied load for one of five vertical positions on the footpad: the center, the upper and lower extremities directly over the junction with the outer beam, and the two halfway points between the center and the extremities.

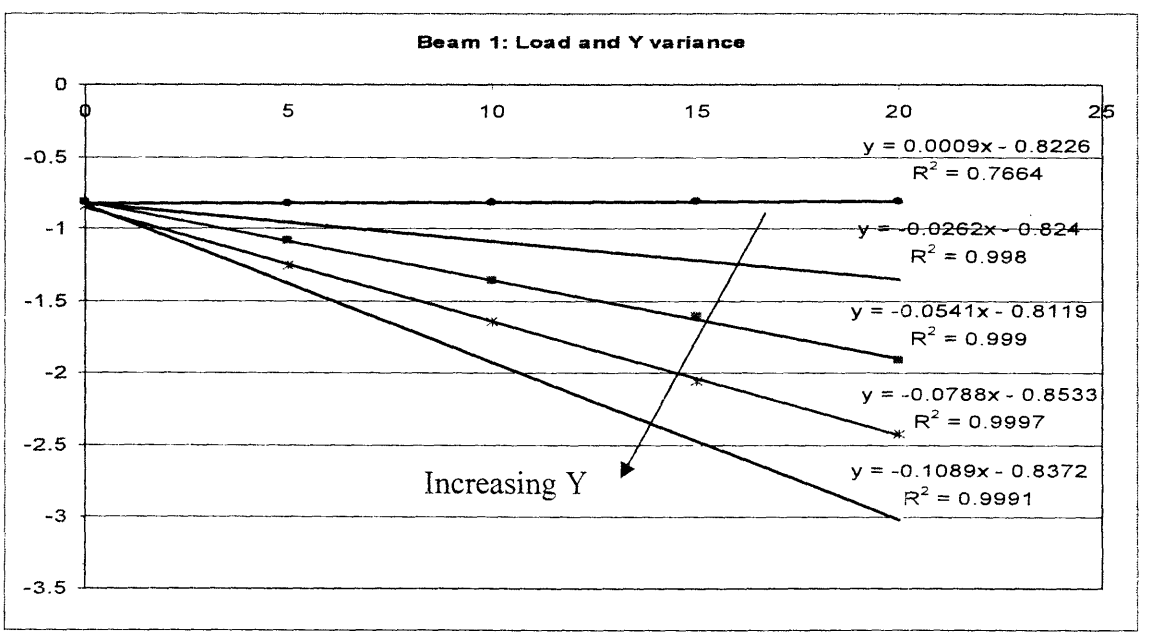

Figure 17: *Center beam response to loads applied at various vertical positions Y.*

The bottommost line corresponds to maximum vertical position, Y: for every load along this line, the vertical position was just above the extremity of the beam being measured. The five points on the line are loads 0, 5, 10, 15, and 20 pounds at that position. The top line corresponds to minimum Y, where the loads were applied at the opposite extremity, and all lines in between are even increments of Y, 1.75 inches from one extremity to the other.

Note that every line with the exception of the first is again very linear, with $R^2 > .99$, verifying that the beams do convert load linearly to output voltage. The top correlation is noisy because there is almost no load on the beam being measured: in this case the load is at the opposite extremity and is born entirely by the opposite beam. This result shows that the two beams are uncoupled – loading one beam has almost no effect on the output of the other beam, in other words F_{c1} has no relationship with F_{c2}.

Because the slopes of the correlations increase linearly with Y, the applied load must also vary linearly with Y. For any applied load, the output voltage varies linearly with vertical position on the footpad.

The bottommost fit, where the load is applied over the beam's juncture with the outer beam, is the one used to calibrate the beam for the field test. For beam 1 the multiplication factor is the slope of the line, -.1089 V / lb and for beam 2, .1009 V / lb.

4.2.2 Center Span Performance

The waveforms for the dynamic compressive loads on each of the center spans during two of the trials are shown in Figure 18 and 19. Note that field test 5 is not shown as its data was approximately the same as field test 6. The irregular data in the first second of the trial corresponds to the set position before the gun. The large spike is the actual start,

and the linear output in the last ½ second corresponds to the blocks returning to their unloaded position.

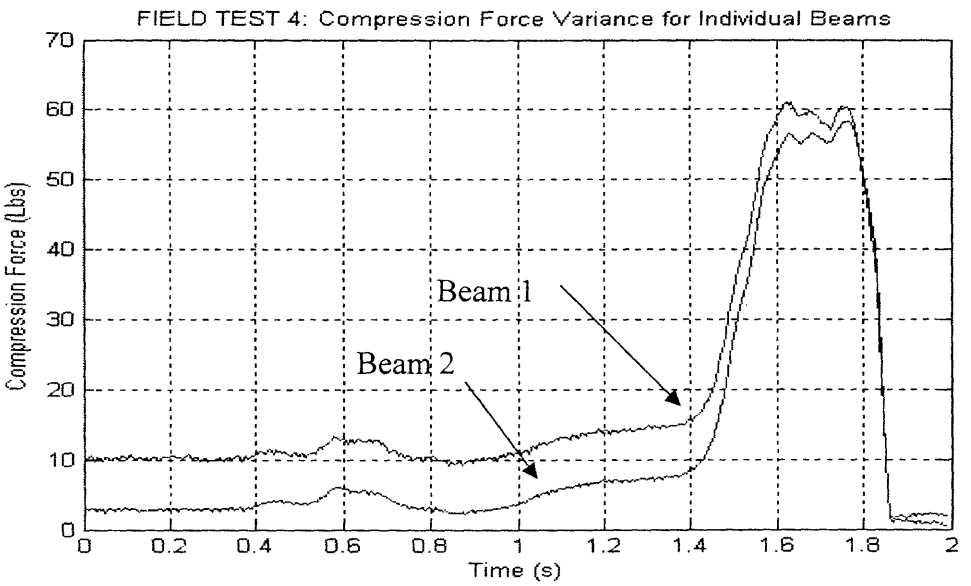

Figure 18: *Responses of both beams in the center span to compressive load during a start.*

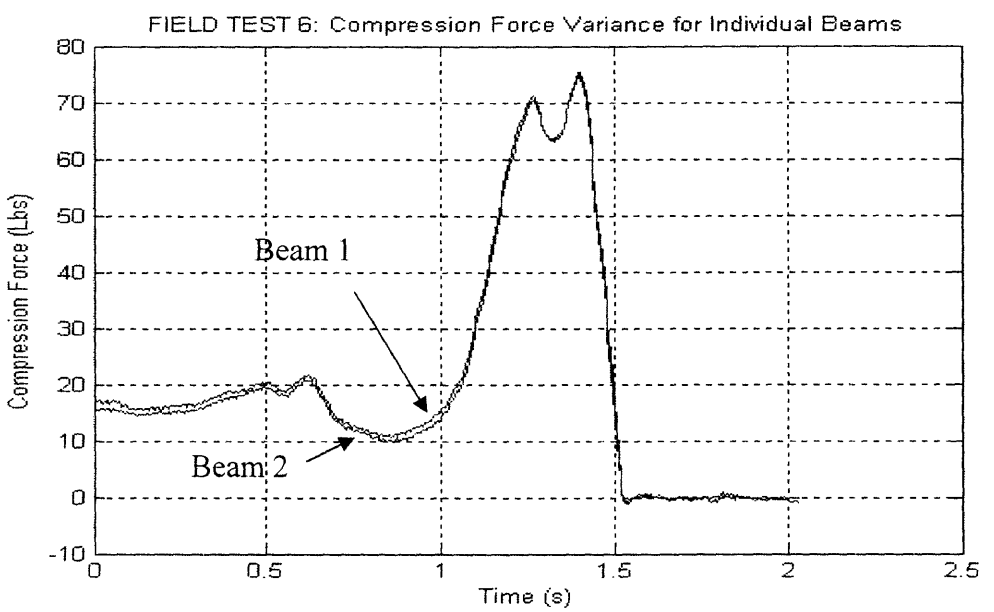

Figure 19: *For another trial, responses of both beams due to compressive load during a start. Beam 1 is above Beam 2.*

From the measurements of the individual beams, the total compression force and the vertical position Y can be calculated via Equation (18).

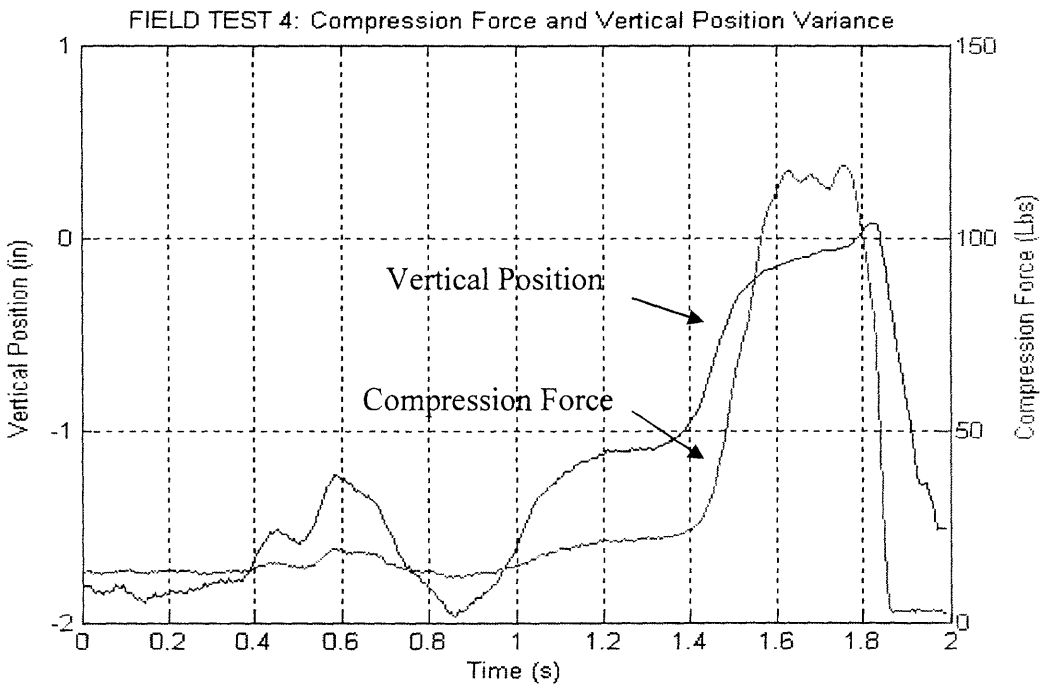

Figure 20: *Total compressive load and vertical position of force calculated from individual measurements of the two beams of the center span.*

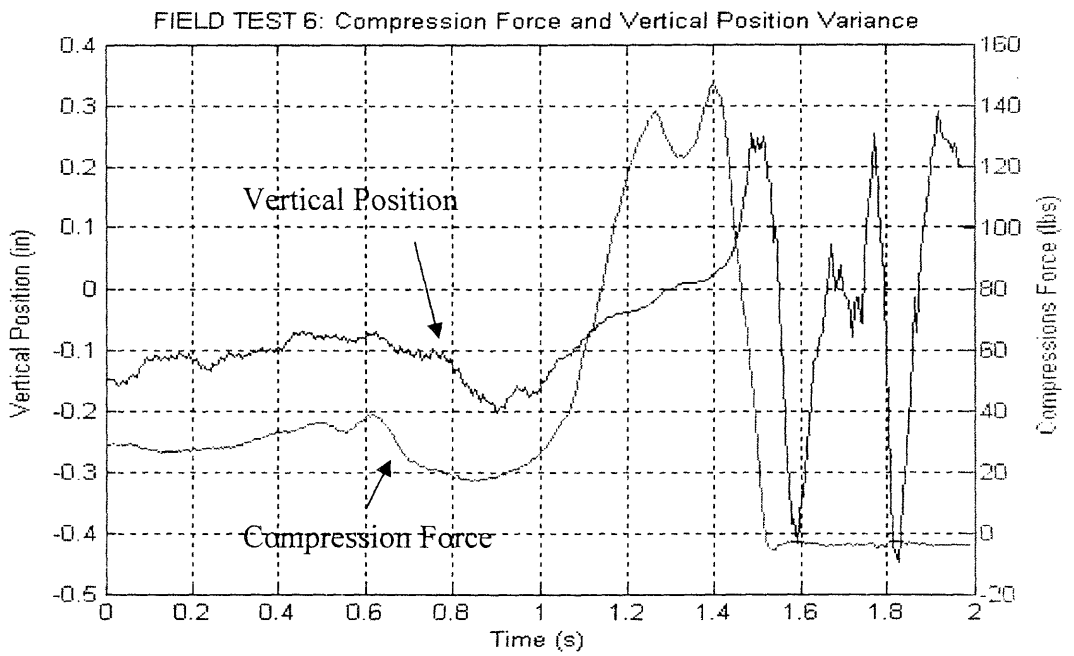

Figure 21: *Again, total compressive load and vertical position of force calculated from individual measurements of the two beams of the center span.*

4.3 Data Interpretation

4 3.1 Graph Shapes

In both trials the duration of the start was very long, nearly 4/10ths of a second as compared to a more typical quarter second or faster. Long start times are an indicator that the athlete may be taking too long of a first stride with his rear leg, forcing him to push on his front leg for a longer period of time. This motion is typical of new sprinters who "hang" their lead arm by driving it out at the gun but not retracting it with enough speed, lengthening their initial step.

The irregularity in the peak force during trial 6 is consistent with the runner's report of his knee buckling mid start. That jerking motion is reflected in the force measurement as a sudden drop in the compression force. The plateau of the peak force during trial 6 suggests that the athlete may have reached the limit of his strength. This particular athlete is able to lift 250 pounds with both legs, so 120 pounds is a reasonable estimation of the limit of a single leg.

In trial 4 the athlete started with his foot resting partially on the floor and partially on the bottom of the footpad, with his heel straight up in the air. The center of force therefore starts below the center axis, since in the marks position the athlete is applying pressure to the lower beam of the flexure. During the start, the center of force moves back to the center of the footpad, suggesting that the athlete's foot flexed about the ankle, moving the heel towards the blocks and bringing more of the upper portion of his foot into contact. The movement of the center of force reflects redistribution of pressure rather than the rolling or sliding of the foot.

4.3.2 Numerical Synthesis

Start Comparison		
	Field Test 4	Field Test 6
Time to Threshold Force (Reaction Time)	1.475 s	1.075 s
Peak Force	118.7 Lbs (528.75 N)	146.9 Lbs (654.37 N)
Time to Peak Force	.285 s	.33 s
Force Duration	.395 s	.485 s
Total Impulse	37.42 Lb-s (166.68 N-s)	47.29 Lb-s (210.65 N-s)
Average Power	94.73 f-Lbs/s (421.99 W)	97.505 f-Lbs/s (434.34 W)
Exit Speed (m=70 kg)	6.89 f/s (2.29 m/s)	8.70 f/s (2.90 m/s)
Generated Acceleration	18.07 f/s^2 (6.02 m/s^2)	18.61 f/s^2 (6.20 m/s^2)
Acceleration Made Good	17.43 f/s^2 (5.80 m/s^2)	17.43 f/s^2 (5.98 m/s^2)

Table 1: *Numerical Synthesis of two sample field tests.*

The quality of the start can be analyzed with the many parameters listed in Table 1. The start is measured from the point at which the compressive load exceeds forty pounds until it returns to zero. This is representative of how the blocks will be used in production: the electronics will not sample data until a certain threshold force is broken. The blocks cannot sample force all the time, so they will have to be triggered by the user to begin sampling before the start. The blocks will then actively sample, and then begin recording and transmitting data only when threshold force is broken. The time to reach the threshold force is essentially the athlete's reaction time: the time it took the athlete to recognize the gun and apply force to the blocks. In the field the blocks will have to have a way of detecting the time of the start. Ultimately the best start is not the start with the highest peak force but the highest average acceleration. Although the athlete in field test 6 applied a greater impulse on the blocks and his exit speed is greater, he also spends more time in the blocks, and has a disadvantage to the more powerful starter in the opposite trial.

In the trials above it is difficult to define the runner's absolute acceleration without taking the force of gravity into account. The footpad is not perpendicular to the ground, so there is some small component of gravity that contributes to the total force. An athlete could tilt the blocks to be more parallel to the ground, and the same load reading could result even if the athlete's horizontal acceleration was less. In the calculation above, the acceleration has been adjusted to take into account the 15 degree angle of the blocks, to give "acceleration made good": the component of the acceleration parallel to the ground. In the field, the blocks may require user input about the angle setting of the footpad in order to render this data.

4 3.3 Verification of Calculated Parameters

Though the 100m race is considered an all out sprint, not even Olympic athletes can sustain their top speed for more than 30 meters. This means that although most 100 meter runners are able to sustain 100% effort for the duration of the race, they are only running at their maximum speed for a short section. In the beginning of the race, obviously, their effort is spent accelerating their weight. In the last 30 or so meters of the race, their speed declines to some percentage of their top speed. Great sprinters therefore run faster times by decreasing the time they need to accelerate (lifting weights to provide greater acceleration) and slowing the decline of their speed at the end of the race (doing endurance workouts to maintain as much speed as possible). The speed profile of a collegiate runner might look like the following:

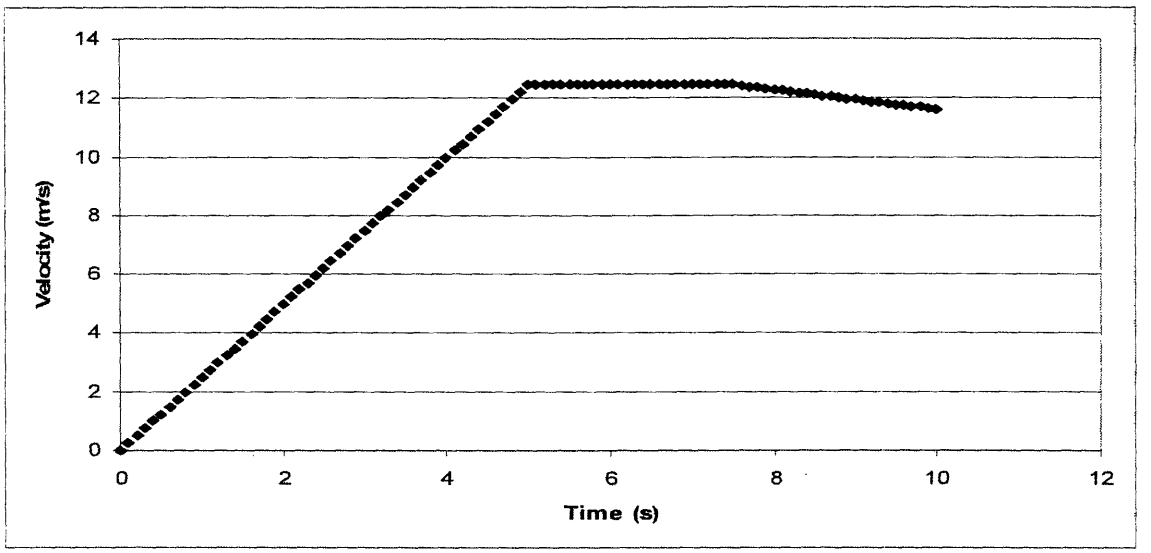

Figure 22: *Sample speed profile for a runner in a 100m sprint. The runner accelerates from the blocks in the first linear portion of the profile, holds his top speed in the second portion, and slowly loses speed in the final portion.*

Here the runner finishes the race in 11.00 seconds. It is assumed that he reaches his top speed after 30 meters, is able to maintain that speed for another 30, and then able to finish the race at 90% of his top speed. Assuming continuous linear changes in speed, then his top speed would be just over 12 meters (roughly 40 feet) per second. His acceleration, if linear, would therefore be 2.49m/s^2 on average over the first 5 seconds of the race. However, since we know that the runner is exerting constant power, not constant acceleration, it would be appropriate to remodel the first portion of his race as shown below:

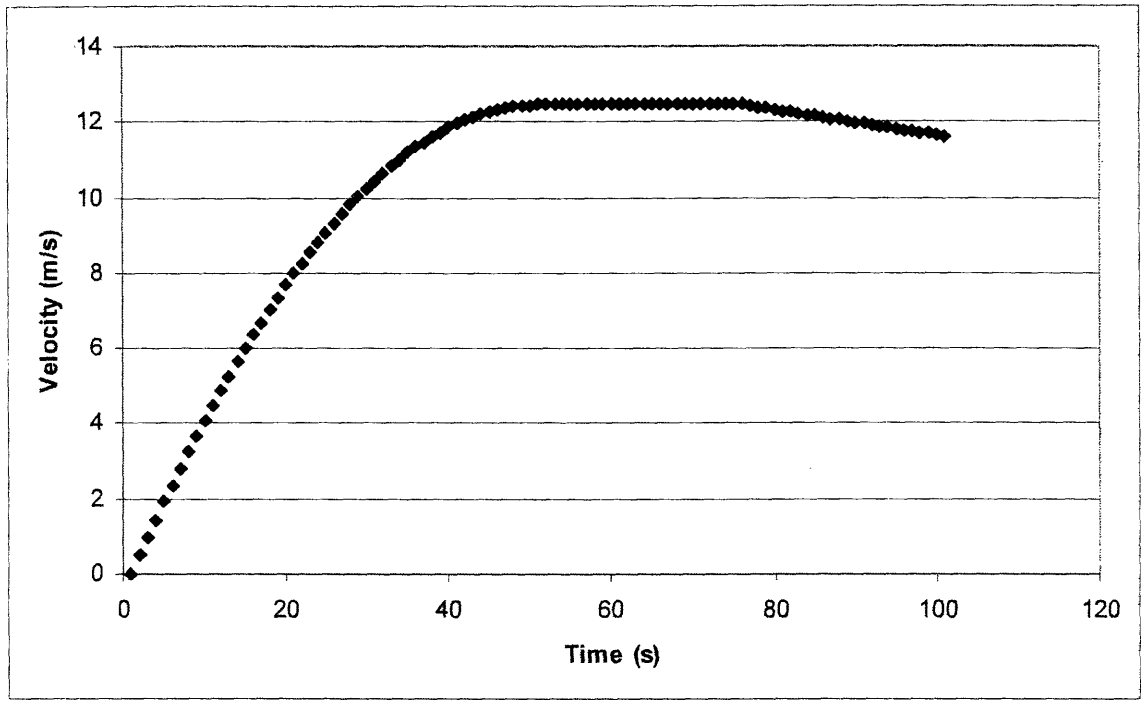

Figure 23: *Revised speed profile for the sprinter. Here his acceleration is sharper at the beginning of the race and approaches top speed more smoothly.*

where his initial acceleration is instead parabolic. This makes sense as the runner should be accelerating his hardest at the very beginning of the race. This rough model calculates the initial acceleration of the sprinter to be 3.84 m/s^2 if he starts from a standing position; of course, his initial acceleration would be even greater if he used blocks. The sprinter tested in field tests 4 and 6 generated average accelerations of 5.80 m/s^2 and 5.98 m/s^2, both plausible measurements when compared to the above theory.

Further Research

There are several opportunities for further research with this project. First and foremost, the electronics interface is being designed that will capture all eight active bridge outputs simultaneously, allowing the transducer to be used to its full potential. The transducer could then be used to measure several characteristics in addition to the three major forces:

1) Fatigue of an athlete over the course of several starts, and how that fatigue correlates to changes in peak force and force duration
2) Performance of an athlete after vigorous exercise such as mileage or lifting
3) Performance variation over long time spans such as months or seasons
4) Performance variations in the presence of other athletes or under stressful conditions such as during gun starts
5) Performance variations with adjustment of the spacing and angle of the footpad
6) Performance differences when an athlete starts with his other foot forward

An interesting experiment might be to construct a second footpad using commercially available force transducers such as S-shaped load cells or load buttons. The data from the two footpads could then be compared and scrutinized.

It might also be worthwhile to revisit some of the engineering decisions that brought the design to where it is. There are a few weaknesses in the design, most noticeably the lateral stiffness and the fragility of the strain gages. The adjustment assembly has some tolerance issues that cause it to shift laterally during hard starts. Although this movement does not affect the data, it is perceived by the user as weakness in strength and can be distracting.

By far the least robust part of this system is the strain gage itself, which despite hardware compensation is still susceptible to noise and environmental effects. The gages

themselves are fragile, since the wires in the measurement array are each susceptible to abrasive contact prior to mounting. Over the course of testing and refinement several gages we mounted properly and soldered before shorting, requiring lengthy and tedious replacement. Attaching the lead wires to the small solder pads is difficult by hand and impossible without flexible (stranded), small gage wire. All the leads must be strain relieved to prevent accidentally dislodging the solder pads from the backing. Even once they are mounted and protected it is difficult to verify the quality of the bond and to project its lifespan of accurate measurement. The glue, though matched to the backing and to the aluminum surface, might creep with time or worse, vary from one production run to the next. Further research might therefore investigate options that sense force via other methods.

Tekscan, Inc is a Cambridge, MA technology company that manufactures a piezoelectric button capable of integrating pressure over a small area. Early in the concept development of this project the Tekscan sensor was considered as a potential solution but rejected because of its cost and Tekscan's propriety over the controlling hardware and software. Piezoelectric film by itself, however, still presents a variety of design options that could alleviate some of the issues described above.

Instead of sensing strain an alternative method of deducing loads might be to detect the deflection of the transducer. There are a slew of technologies capable of this type of measurement, though fragility and availability of power sources may preclude their use.

Conclusions

The transducer design was successful in its ultimate goal of capturing force and position data from an actual race start in the field. The prototype verifies the ability of strain gages to capture relatively small loads with great accuracy, linearity, and repeatability, with only small effects due to background interference.

The transducer also accomplished its goals of adding new capability and functionality over the existing products on the market. The transducer does output forces in concrete units, is able to generate independent data for each foot, and is further able to deduce forces in directions in addition to the normal.

The overall cost of production, however, could be prohibitive to eventual mass manufacturing. Strain gages, the critical component of the transducer, turned out more expensive than initially anticipated, driving the cost of the transducer upwards of 100 dollars in materials alone. Although the production version will benefit from economy of sale, the cost of having the gages mounted by a third party will more than make up the difference. The cost of materials and labor, in addition to the cost of necessary electronics downstream of the Wheatstone bridges and amplifiers could push the total manufacturing cost above the target of $500. This additional unit cost will make it difficult to market the product against established competitors in the field.

References

Ashby, Michael F. Materials Selection in Mechanical Design, Second Edition. Jordan Hill Oxford: Butterworth and Heinman, 1999.

I W Hunter and BJ Hughey. Muscle Force Experiment, Soda Can Experiment 2003

Khan, Akhtar S, and Wang, Kinwei. Strain Measurements and Stress Analysis. Upper Saddle River New Jersey: Prentice Hall, 2001.

Murray, William M and Miller, William. The Bonded Electrical Strain Gage, an Introduction. New York and Oxford: Oxford University Press, 1992.

Oberg, Erik, Jones Franklin. Machinery's Handbook, 26th Edition. New York New York: Industrial Press, Inc 2001.

Window, A L. Strain Gauge Technology, Second Edition. London and New York: Elsevier Science Publishers LTD, 1992.

Appendix A: Mechanical Drawings

ITEM NO.	DESCRIPTION	QTY.
1	Footpad Base	1
2	Force Transducer	1
3	Flexure Mount	1
4	Foot Plate	1
5	Enclosure	1
6	Mount Adjuster	1
7	D Sub Connector	1
8	Support Pegs	1
9	1/4 20 x 1inch Bolt	1
10	1/4 20 Lock Nut	1
11	#10-24 .75 inch Bolt	2
12	#10-32 .5 inch Flathead	2
13	#10-32 1 inch Pan Head	4
14	#10 Washer	4
15	#10-32 Nut	4

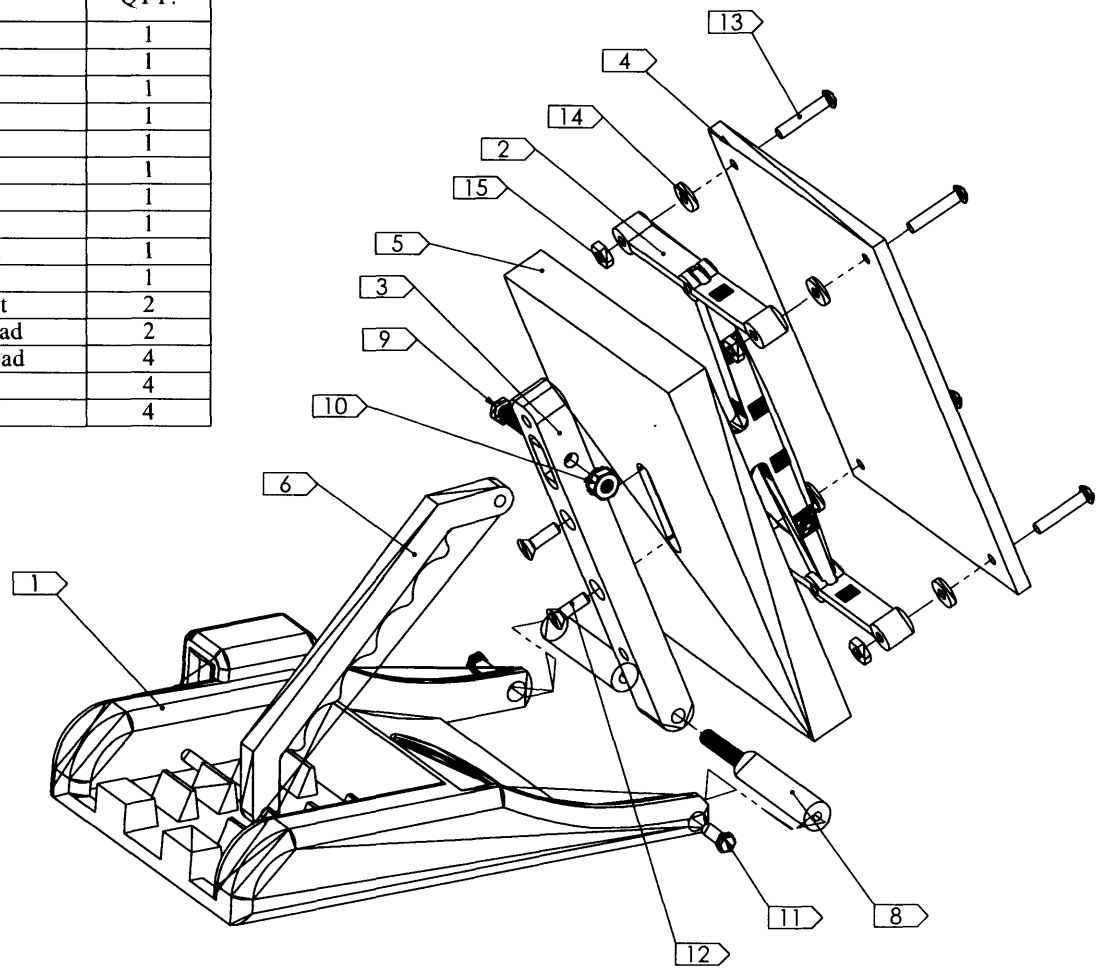

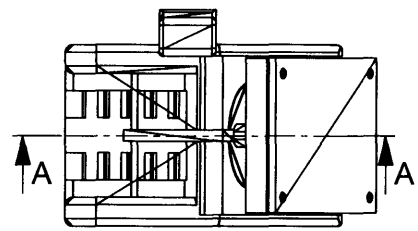

TOP

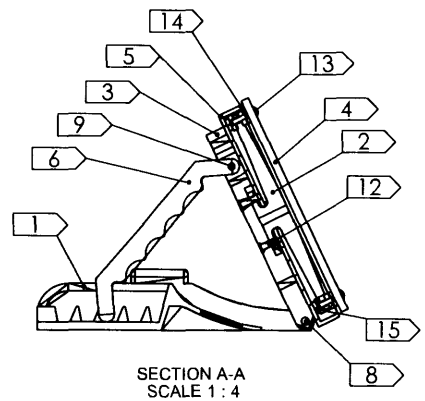

SECTION A-A
SCALE 1 : 4

97 Bay State Road
Boston MA, 02215
P. 617.852.5505
E. ztraina@mit.edu

MATERIAL:	
FINISH:	
WEIGHT:	
VOLUME:	
DRAWING BY	Zach Traina
CHECKED BY	

UNLESS OTHERWISE SPECIFIED
1. REMOVE ALL BURRS AND SHARP EDGES
2. ALL DIMS IN INCHES (MM)
LIN. TOL: .X ± .1" .XX ± .01" .XXX ± .004"
ANG. TOL: .A ± 1° .AA ± .1° .AAA ± .01°

DRAWING FILE: File name assy Created by Zach Tuesday, May 03, 2005 10:21:30 PM Last saved Tuesday, May 03, 2005 10:58:15 PM
MODEL FILE File Name Full Side mod Created by Zach Thursday, February 24, 2005 11:04:20 PM Last saved Tuesday, May 03, 2005 10:57:01 PM

PART DESCRIPTION: **Footpad Assembly** | REV: **AA.05**

Fabrication Dimensions | REV: 1 | SCALE: 1:2 | Sheet 1 of 1

CLASS | PROJECT: **2.Thu Undergrad Thesis**

Printed 5/3/2005

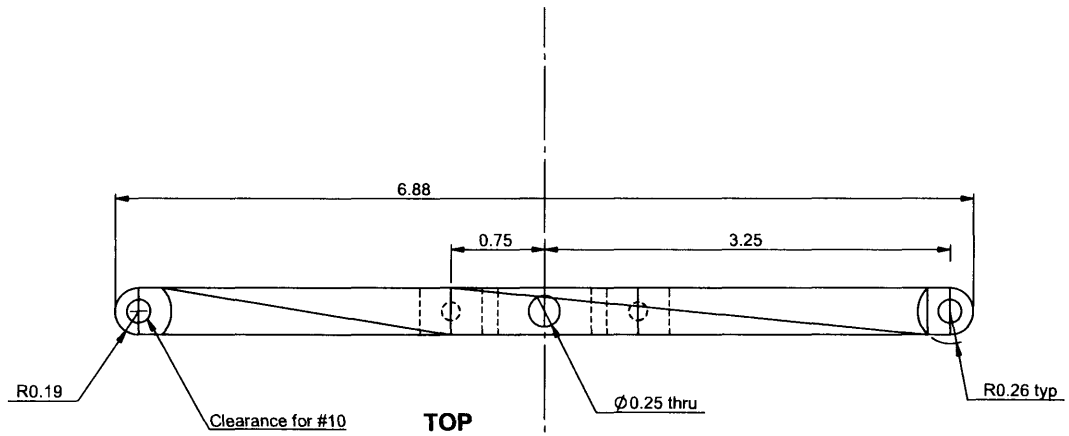

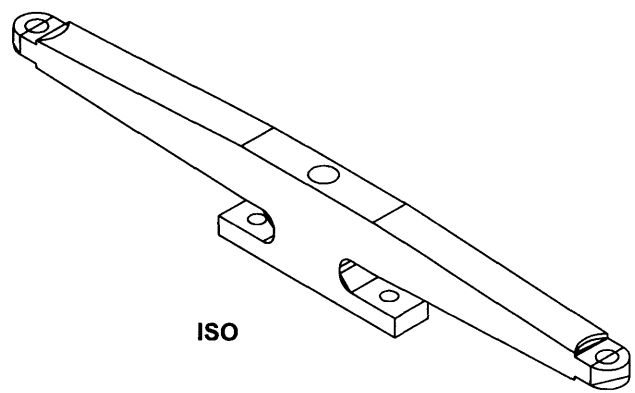

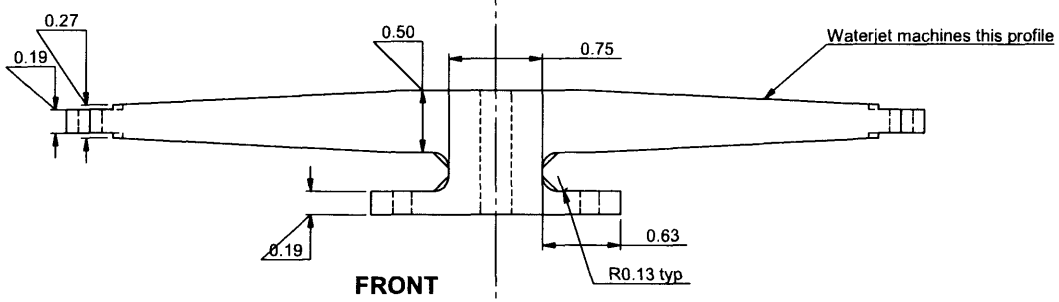

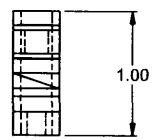

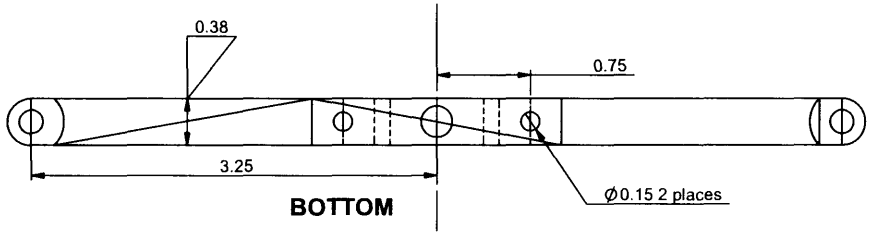

97 Bay State Road
Boston MA, 02215
P. 617.852.5505
E. ztraina@mit.edu

MATERIAL:	6061 Alloy
FINISH:	
WEIGHT:	0.11
VOLUME:	1.16
DRAWING BY	Zach Traina
CHECKED BY	

UNLESS OTHERWISE SPECIFIED
1. REMOVE ALL BURRS AND SHARP EDGES
2. ALL DIMS IN INCHES (MM)
LIN. TOL: X ± 1" .XX ± .01" .XXX ± .004"
ANG. TOL: .A ± 1° .AA ± .1° AAA ± .01°

DRAWING FILE: File name Center flexureCreated by Zach Monday, March 07, 2005 2:11:33 PM Last saved Monday, May 02, 2005 9:57:49 PM

MODEL FILE File Name center flexure Created by Zach Thursday, February 24, 2005 6:47:35 PM Last saved Sunday, May 01, 2005 2:05.00 PM

PART DESCRIPTION: **Center Flexure** | REV: **AA.01**

Fabrication Dimensions | REV: 2 | SCALE: 1:2 | Sheet 1 of 2

CLASS

PROJECT: **2.Thu Undergrad Thesis**

Printed 5/2/2005

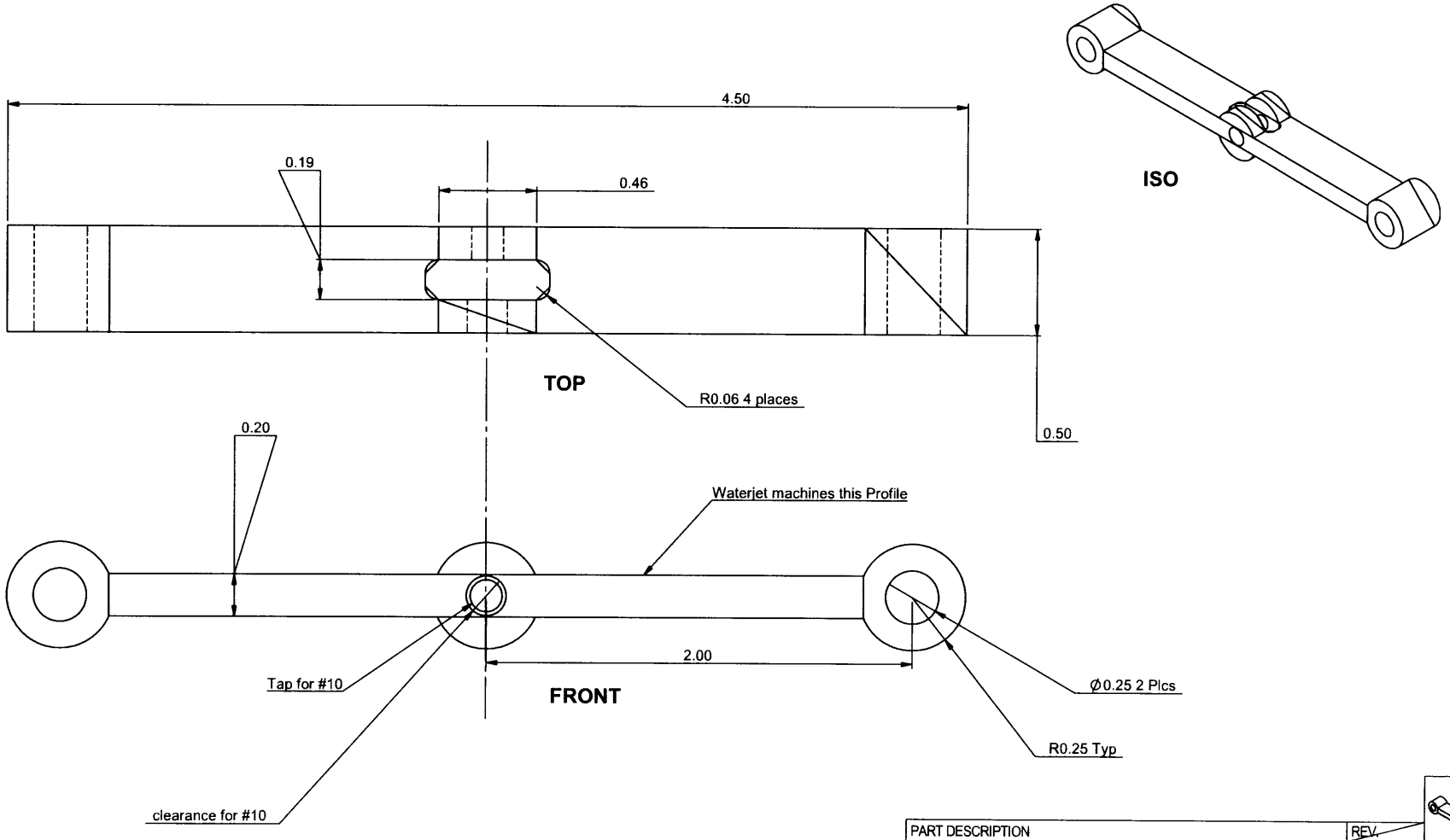

97 Bay State Road
Boston MA, 02215
P. 617.852.5505
E. ztraina@mit.edu

MATERIAL:	6061 Alloy
FINISH:	
WEIGHT:	0.05
VOLUME:	0.50
DRAWING BY	Zach Traina
CHECKED BY	

UNLESS OTHERWISE SPECIFIED
1. REMOVE ALL BURRS AND SHARP EDGES
2. ALL DIMS IN INCHES (MM)
LIN. TOL: .X ± .1" .XX ± .01" .XXX ± .004"
ANG. TOL: .A ± 1° .AA ± .1° .AAA ± .01°

DRAWING FILE: File name End Flexure Created by Zach Monday, March 07, 2005 2:30:05 PM Last saved Monday, May 02, 2005 9:50:03 PM

MODEL FILE File Name end flexure Created by Zach Thursday, February 24, 2005 7:26:51 PM Last saved Monday, April 25, 2005 8:36:16 PM

Printed 5/2/2005

PART DESCRIPTION: **End Flexure** REV: **AA.01**

Fabrication Dimensions REV: 2 SCALE: 2:1 Sheet 1 of 2

CLASS

PROJECT: **2.Thu Undergrad Thesis**

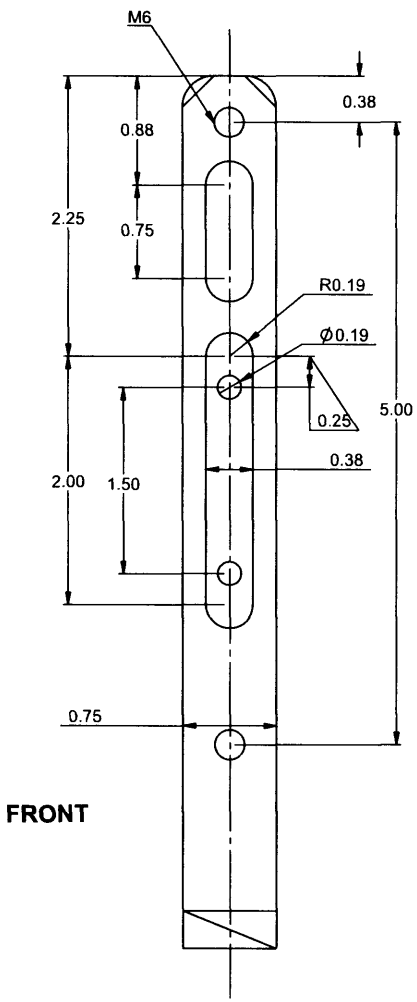

FRONT

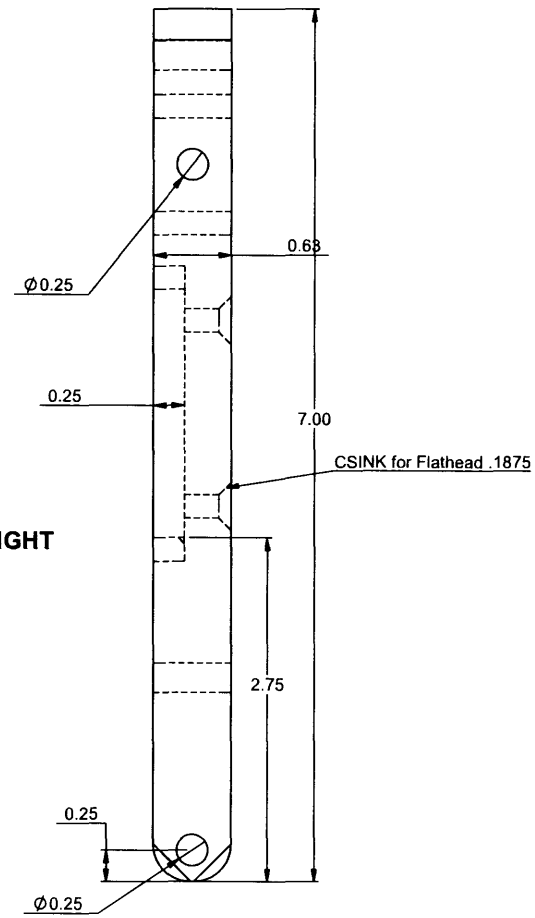

RIGHT

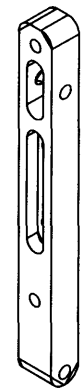

ISO

PART DESCRIPTION: **Flexure Mount** | REV: **AA.02**

Fabrication Dimensions | REV: 2 | SCALE: 1:2 | Sheet 1 of 1

CLASS | PROJECT: **2.THu Undergrad Thesis**

PROPRIETARY AND CONFIDENTIAL

THIS DRAWING CONTAINS PROPRIETARY INFORMATION AND SHALL NOT BE USED, REPRODUCED, OR DISCLOSED TO THIRD PARTIES WITHOUT WRITTEN AUTHORIZATION.

97 Bay State Road
Boston MA, 02215
P. 617.852.5505
E. ztraina@mit.edu

MATERIAL:	6061 Alloy
FINISH:	
WEIGHT:	0.26
VOLUME:	2.64
DRAWING BY	Zach Traina
CHECKED BY	

UNLESS OTHERWISE SPECIFIED
1. REMOVE ALL BURRS AND SHARP EDGES
2. ALL DIMS IN INCHES (MM)
LIN. TOL: .X ± .1" .XX ± .01" .XXX ± .004"
ANG. TOL. A ± 1° .AA ± .1° .AAA ± .01°

DRAWING FILE: File name flexure mount Created by Zach Monday, April 11, 2005 11:01:05 AM Last saved Tuesday, May 03, 2005 8:31:40 PM

MODEL FILE File Name adjusment plate mod Created by Zach Thursday, February 24, 2005 11:16:04 PM Last saved Tuesday, May 03, 2005 8:29:38 PM

Printed 5/3/2005

NOTES:

Thickness .375
Thru post .Ø25" 5"

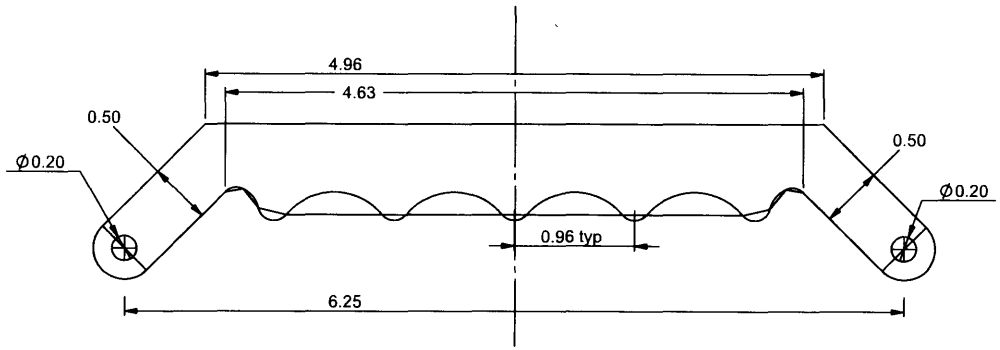

FRONT

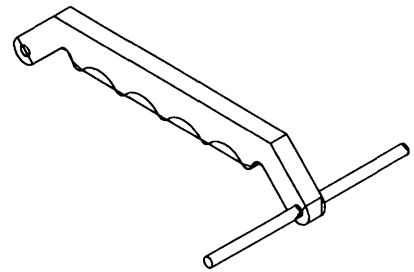

ISO

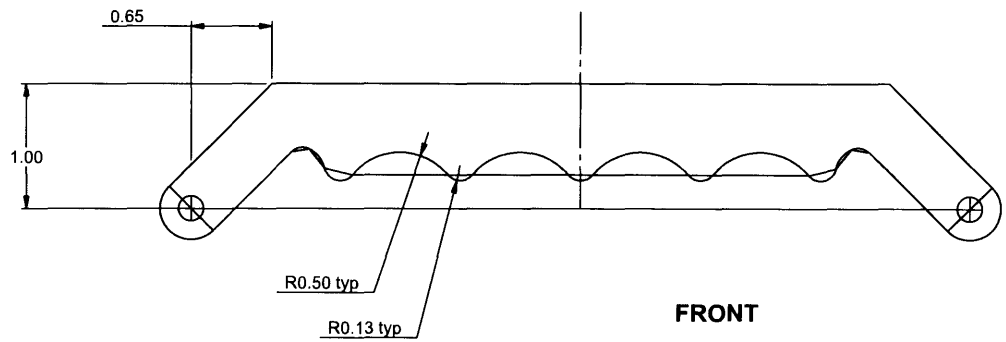

FRONT

PART DESCRIPTION	Mount Adjuster
REV.	AA.01
	Fabrication Dimensions
REV:	2
SCALE:	1:2
Sheet	1 of 1
CLASS	
PROJECT	2.THu Undergrad Thesis

97 Bay State Road
Boston MA, 02215
P. 617.852.5505
E. ztraina@mit.edu

MATERIAL:	6061 Alloy
FINISH:	
WEIGHT:	0.17
VOLUME:	1.71
DRAWING BY	Zach Traina
CHECKED BY	

UNLESS OTHERWISE SPECIFIED
1. REMOVE ALL BURRS AND SHARP EDGES
2. ALL DIMS IN INCHES (MM)
LIN TOL: .X ± .1" .XX ± .01" .XXX ± .004"
ANG. TOL: .A ± 1° .AA ± .1° .AAA ± .01°

DRAWING FILE: File nameMount AdjusterCreated by Zach Monday, April 11, 2005 11:41:13 AM Last saved Monday, May 02, 2005 10:06:00 PM

MODEL FILE File Name Support mod Created byztraina Wednesday, March 30, 2005 2:18:19 AM Last saved Tuesday, April 12, 2005 12:17:24 PM

Printed 5/2/2005

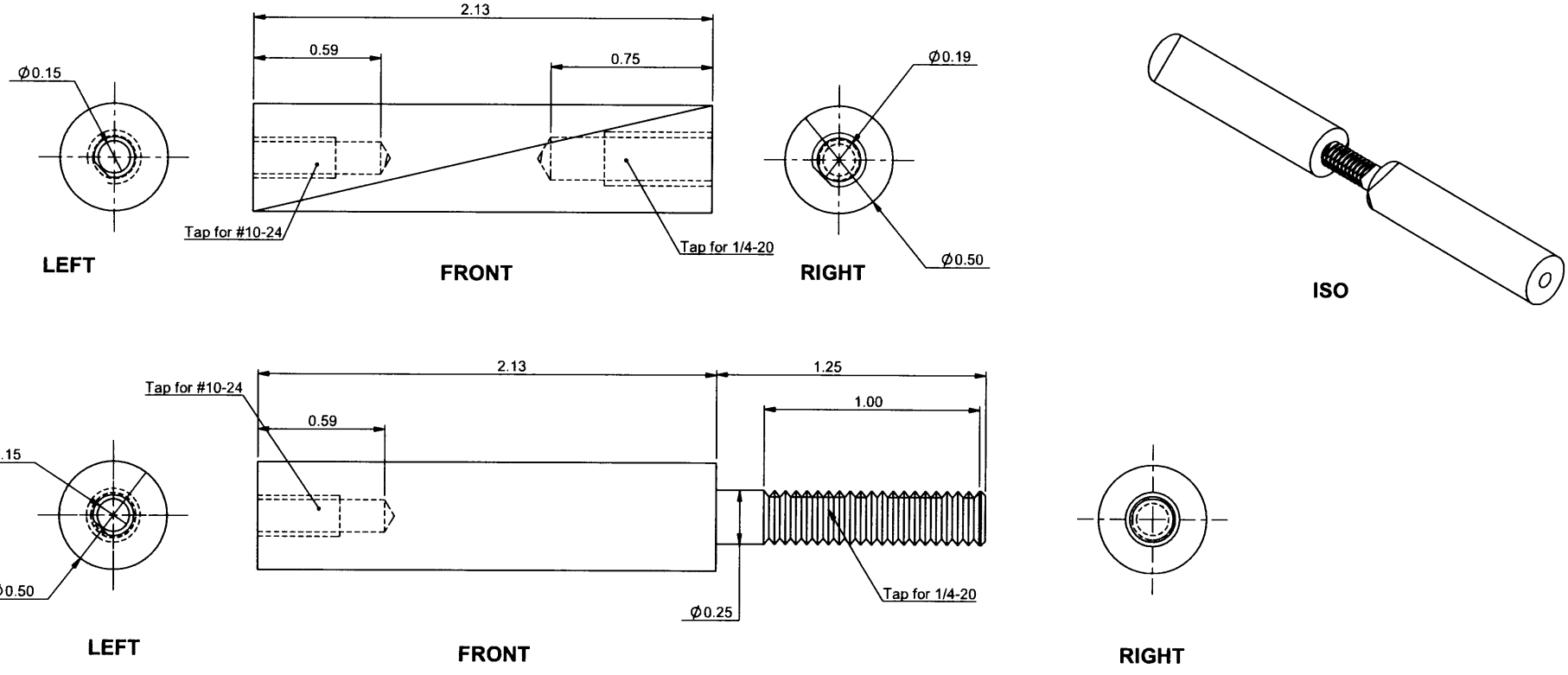

PROPRIETARY AND CONFIDENTIAL

THIS DRAWING CONTAINS PROPRIETARY INFORMATION AND SHALL NOT BE USED, REPRODUCED, OR DISCLOSED TO THIRD PARTIES WITHOUT WRITTEN AUTHORIZATION.

97 Bay State Road
Boston MA, 02215
P. 617.852.5505
E. ztraina@mit.edu

MATERIAL:	Aluminum 6061 T6
FINISH:	
WEIGHT:	
VOLUME:	
DRAWING BY	Zach Traina
CHECKED BY	

UNLESS OTHERWISE SPECIFIED
1 REMOVE ALL BURRS AND SHARP EDGES
2 ALL DIMS IN INCHES (MM)
LIN. TOL: .X ± .1" .XX ± .01" .XXX ± .004"
ANG. TOL .A ± 1° .AA ± .1° .AAA ± .01°

DRAWING FILE: File name pegs Created by Zach Tuesday, May 03, 2005 8:41:52 PM Last saved Tuesday, May 03, 2005 8:57:34 PM

MODEL FILE File Name pegs Created by Zach Tuesday, May 03, 2005 8:48:11 PM Last saved Tuesday, May 03, 2005 8:55:21 PM

Printed 5/3/2005

PART DESCRIPTION: **Support Pegs** REV: **AA.01**

Fabrication Dimensions REV: SCALE: 2:1 Sheet 1 of 1

CLASS

PROJECT **2.Thu Undergrad Thesis**

Appendix B Executive Summary

The objective of this thesis is the design and implementation of a multi-axis force transducer to be integrated into a set of track and field starting blocks. The feedback from this transducer can be used by athletes and coaches to analyze race starts, with the intention of maximizing the runner's speed and power while decreasing wasted side loads and torques. This thesis describes the design of the transducer itself and the supporting infrastructure that connects it to an existing pair of track starting blocks. The transducer is tested in several field trials and generates a measurable voltage output that varies linearly with applied load and loading position. Data collected from the field trials is further analyzed to give insight into the starting mechanics of a collegiate sprinter.

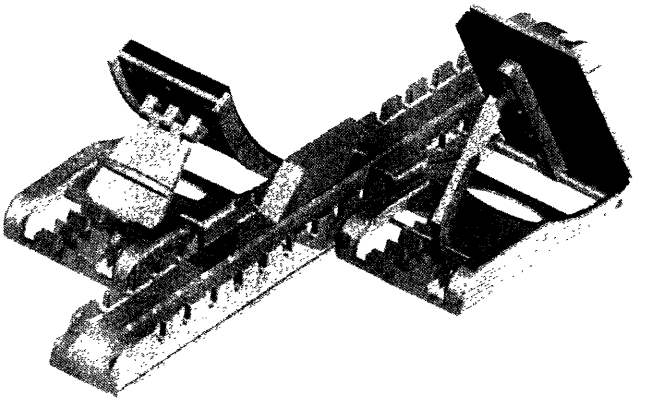

Figure 1: *Modified track blocks displaying the original footpad at left and the enhanced footpad at the right. The modified footpad on the right contains the embedded force transducer.*

This system takes a fundamentally new approach to measuring the forces of an athlete's start by imbedding a flexure within each foot pad. This system is able to measure forces directly and in concrete units instead of inferring abstract force measurements from forces that propagate through the blocks. The embedded measurement system is capable of recording forces in several directions in addition to the horizontal, and is further able to deduce the location

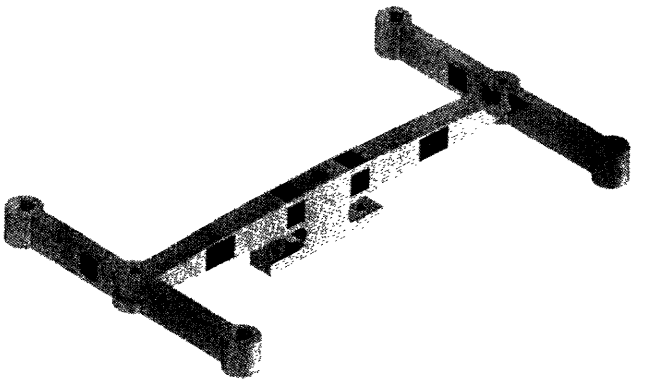

Figure 2: *This embedded flexure uses strain gages to act as a force transducer. Together the gages detect the three major components of the net applied force as well as its position.*

of the center of force during push off, giving more comprehensive and more complete data about each start. Wireless supporting electronics do away with the long and complicated set-up time and make this set-up a fully portable and easily deployable starting solution.

The design consists of four major subassemblies: the *footplate*, the interface that contacts the runner's shoe, the *adjustment plate* which supports the foot plate and adjusts its angle with respect to the ground, the *enclosure* assembly which protects the electronics and the transducer, and the *transducer* itself, which measures the imparted forces. The transducer measures the compressive load applied normal to the footpad, the side load applied horizontally, and the end load applied vertically, as well as the position of the center of force.

After several iterations the design of the transducer settled on bending beams for their sensitivity to light loads, specifically forces less than 400 lbs. Typical axial force transducers are designed to accommodate loads upwards of thousands of pounds. Modifying these existing designs to take light loads would have meant thinning down some sections so small that they would perform well in tension but buckle under any compressive or side load. Bending beams have the advantage of being relatively large (on the order of .5 inch thick) while still being able to produce large strains in response to loading by concentrating stress in the outmost fibers of the beam.

The two center spans are responsible for detecting the magnitude of the compressive and horizontal loads as well as the position of the center of force. Because these beams are insensitive to axial loads, additional beams are mounted at the end of each center span in order to register the end loads with better accuracy. Predictions of applied loading were taken from a study of starting mechanics done by Halston Taylor, coach of the MIT track team, in 1995. In his study the heaviest compressive load by an athlete during a start was 150 kg, ranging down to 70 kg for lighter and weaker athletes. Thus the design is tuned to this range of forces with the ability to withstand forces upwards of 200 kg and the sensitivity to detect loading to within 1 kg anywhere in the range from 0-200kg. The

transducer is tuned for off axis loads approximately 10% of those in compression, though the transducer could withstand and accurately measure forces up to 50% of the compressive load before risking plastic deformation. Results from a field trial are shown below. The green line corresponds to the total compressive load applied to the footpad, and the blue line corresponds to the vertical position of the center of force.

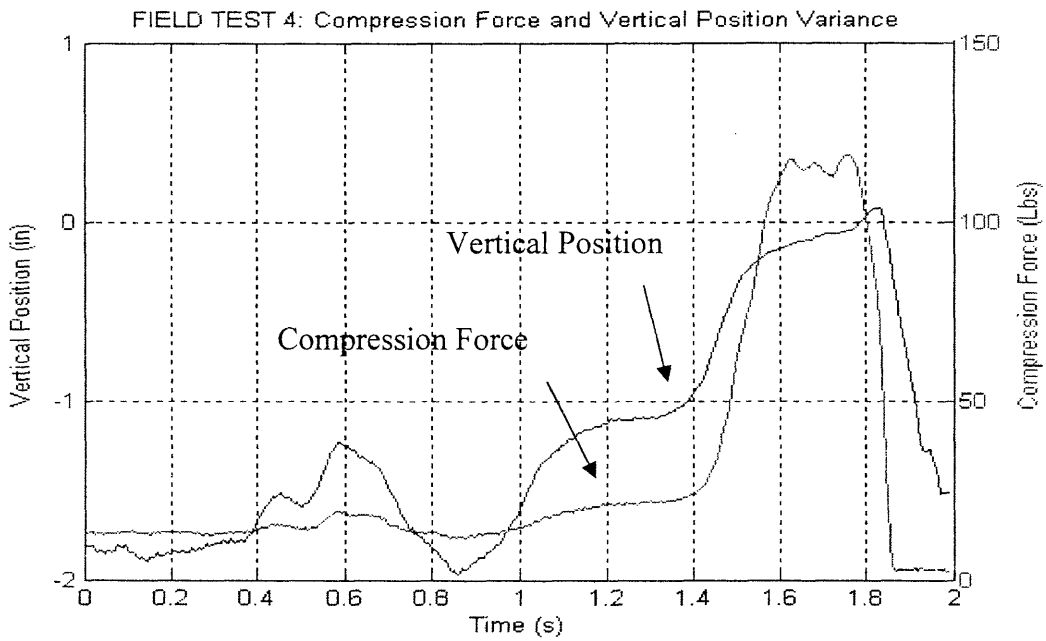

Figure 3: *Total load its vertical position applied by a sprinter during a start.*

There are several opportunities for further research with this project. First and foremost, the electronics interface is being designed that will capture all eight active bridge outputs simultaneously, allowing the transducer to be used to its full potential. The transducer could then be used to measure several characteristics in addition to the three major forces:

1) Fatigue of an athlete over the course of several starts, and how that fatigue correlates to changes in peak force and force duration
2) Performance of an athlete after vigorous exercise such as mileage or lifting
3) Performance variation over long time spans such as months or seasons

4) Performance variations in the presence of other athletes or under stressful conditions such as during gun starts
5) Performance variations with adjustment of the spacing and angle of the footpad
6) Performance differences when an athlete starts with his other foot forward

The transducer design was successful in its ultimate goal of capturing force and position data from an actual race start in the field. The prototype verifies the ability of strain gages to capture relatively small loads with great accuracy, linearity, and repeatability, with only small effects due to background interference. The transducer also accomplished its goals of adding new capability and functionality over the existing products on the market. The transducer provides output forces in concrete units, is able to generate independent data for each foot, and is further able to deduce forces in directions in addition to the normal.

The overall cost of production, however, could be prohibitive to eventual mass manufacturing. Strain gages, the critical component of the transducer, turned out more expensive than initially anticipated, driving the cost of the transducer upwards of 100 dollars in materials alone. Although the production version will benefit from economy of sale, the cost of having the gages mounted by a third party will more than make up the difference. The cost of materials and labor, in addition to the cost of necessary electronics downstream of the Wheatstone bridges and amplifiers could push the total manufacturing cost above the target of $500. This additional unit cost will make it difficult to market the product against established competitors in the field.